SAND2018-XXXX

SAND2018-7391C

# Nanoparticles and Zeolites for Environmental Applications

Tina M. Nenoff,* Leo J. Small,*
Karena W. Chapman, Peter J. Chupas,
Haiyan Zhao, Kevin A. Beyer

*Chemical, Physical, Nano Sciences Center
Sandia National Laboratories
Albuquerque, NM USA

Advanced Photon Source, Argonne National Laboratory, USA

Sandia National Laboratories is a multimission laboratory managed and operated by National Technology and Engineering Solutions, LLC., a wholly owned subsidiary of Honeywell International, Inc., for the U.S. Department of Energy's National Nuclear Security Administration under contract DE-NA-0003525.

Work performed at Argonne and use of the Advanced Photon Source were supported by the U.S. Department of Energy (DOE), Office of Science, Office of Basic Energy Sciences, under Contract No. DE-AC02-06CH11357.

# The Capture and Storage of Iodine Species

Programmatic / Background

Materials of Interest

Zeolites, MOFs, carbons

Nanoparticle Formation and fission gas capture in zeolites

Novel Sensor development and testing in real world conditions

# Outline

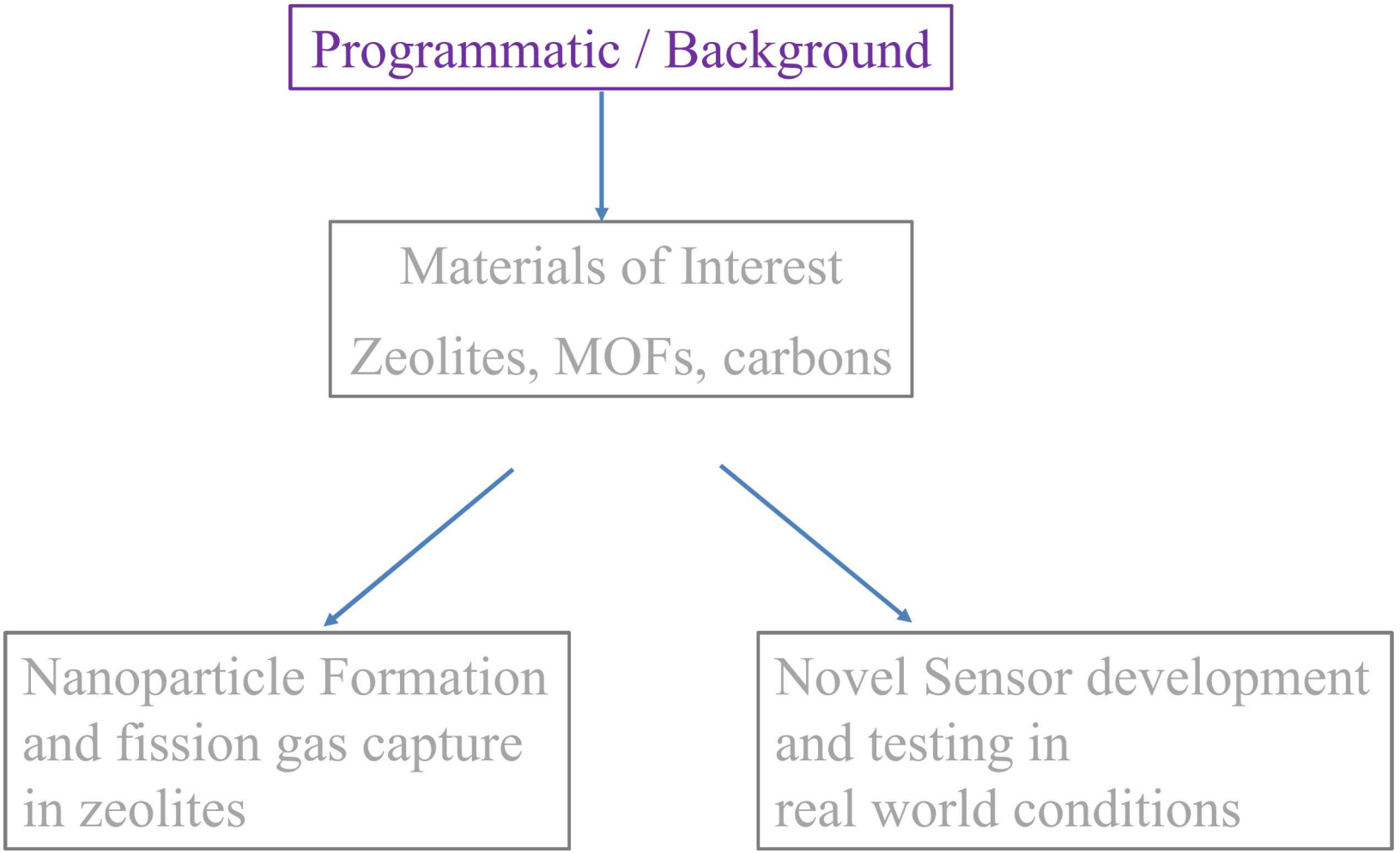
Programmatic / Background
Materials of Interest
Zeolites, MOFs, carbons
Nanoparticle Formation and fission gas capture in zeolites
Novel Sensor development and testing in real world conditions

# Nanoporous Materials (Zeolites, Molecular Sieves & MOFs), Radiological Ion and Gas Capture

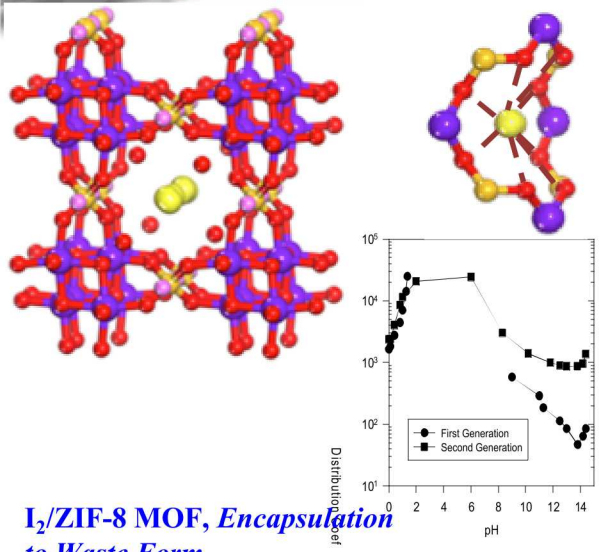


**$I_2$/ZIF-8 MOF, *Encapsulation to Waste Form***
*JACS*, 2011,*133(32)*,12398
*JACS* 2013, *135*, 16256

**CST, Molecular Sieve:**
R&D100 1996
*JACerS*, 2009, *92(9)*, 2144
*JACerS*, 2011, *94(9)*, 3053
*Solvent Extr. & Ion Exch*, 2012, *30*, 33

***CST, $Cs^+$ removal from water to Pollucite Waste Form***
US Patents *6,479,427; 6,110,378*

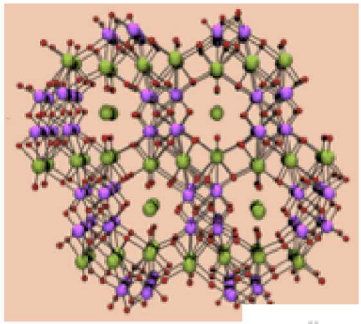

**SOMS Molecular Sieve,**
***$Sr^{2+}$ getter,***
***1-step to Perovksite WF***
*JACS*, 2002,*124(3)*, 1704
US Patent *7,122,164;* 2006

***Fundamental Research to Applied to Commercial Products***
***Design the Separation Material To Develop the Waste Form***

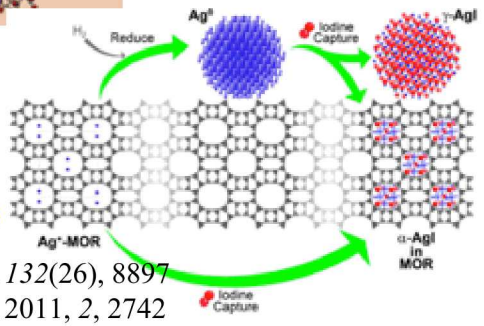


**Ag-MOR Zeolite, *$I_2$(g) capture & mechanisms***
*JACS*, 2010, *132*(26), 8897
*JPC Letters*, 2011, *2*, 2742

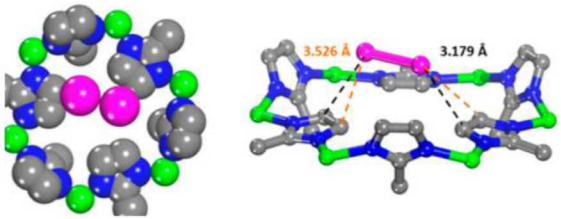


**MOF *Amorphization for Gas Storage***
*JACS*, 2011,*133*(46),18583
US Patent *9,162,914;* 2015

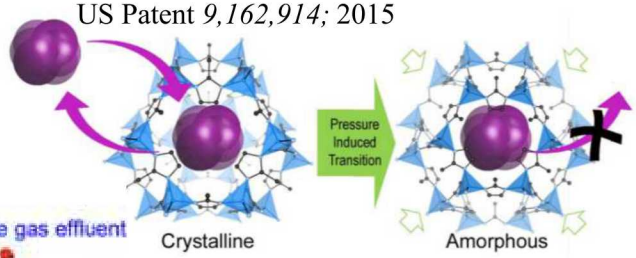


**Org-I; Ag-MOR Zeolite**
*MMM*, **2014**, *200*, 297

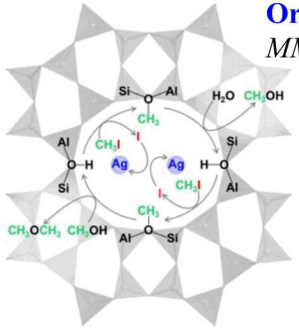

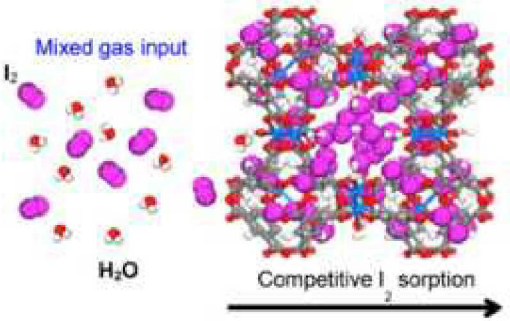


**MOF Cu-BTC*: $I_2$ from Humid Gas Stream***
*Chem. Mater*. 2013, *25*(13), 2591

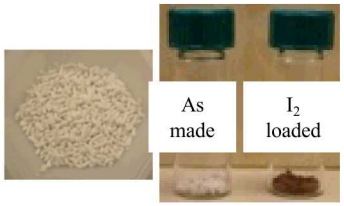


***Binder Free* MOF *Pelletization***
US Patent Pending 2014

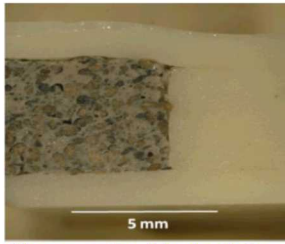


**Glass Composite Materials:**
***Universal Core-Shell Iodine Glass Waste Form & Getter***
*JACerS*, 2011, *94*(8), 2412
US Patent *8,262,950*; 2012

# Pair Distribution Function (PDF) Analysis:
## *To see what is happening inside the pores*

Use of high energy synchrotron:
high energy X-rays and large area detectors key to structure resolution of heavier elements such as *Silver*

*The PDF,* ***G(r)****,* is related to the ***probability*** of finding an atom at a distance ***r*** from a reference atom.
It is the Fourier transform of the total structure factor, ***S(Q)***.

$$\boldsymbol{G(r)} = 4\pi r\,\rho_0[\boldsymbol{g(r)}\text{-}1] = (2/\pi)\int Q[\boldsymbol{S(Q)} - 1]\sin(Qr)\mathrm{d}Q$$

probability — structure factor

The structure factor, ***S(Q)***, is related to coherent part of the diffraction intensity

$$\boldsymbol{S(Q)} = 1 + [\boldsymbol{I^{coh}(Q)} - \sum c_i|f_i(Q)|^2]/\ |\sum c_i f_i(Q)|^2$$

diffraction intensity (corrected)

Apply corrections for background, absorption, Compton & multiple scattering

# PDF measurements: APS/ANL Collaboration

Does it matter which synchrotron?

*Yes. Only higher energy storage rings produce significant fluxes of high energy X-rays*

High energy X-rays are a unique strength of the *Advanced Photon Source* (in the western hemisphere)

- 3 dedicated high energy beam lines
- 1 dedicated PDF beamline

APS 11-ID-B: Dedicated PDF facility
- 58 or 90KeV high energy X-rays
- typical wavelengths = 0.1 - 0.2Å

For our experiments:

$Q > 20Å^{-1}$; $CuK_\alpha$ to $2\Theta = 180$ results in $Q_{max} = 8Å$

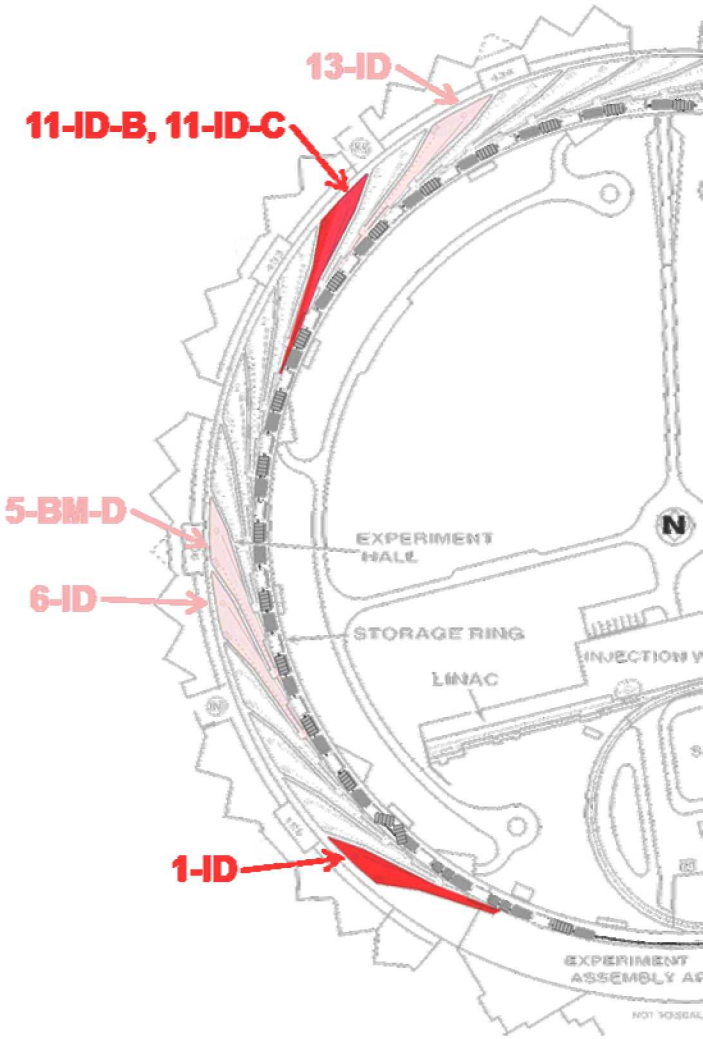

# PDF Provides Insight Into Short Range Structural Order

*- a weighted histogram of ALL atom-atom distances*

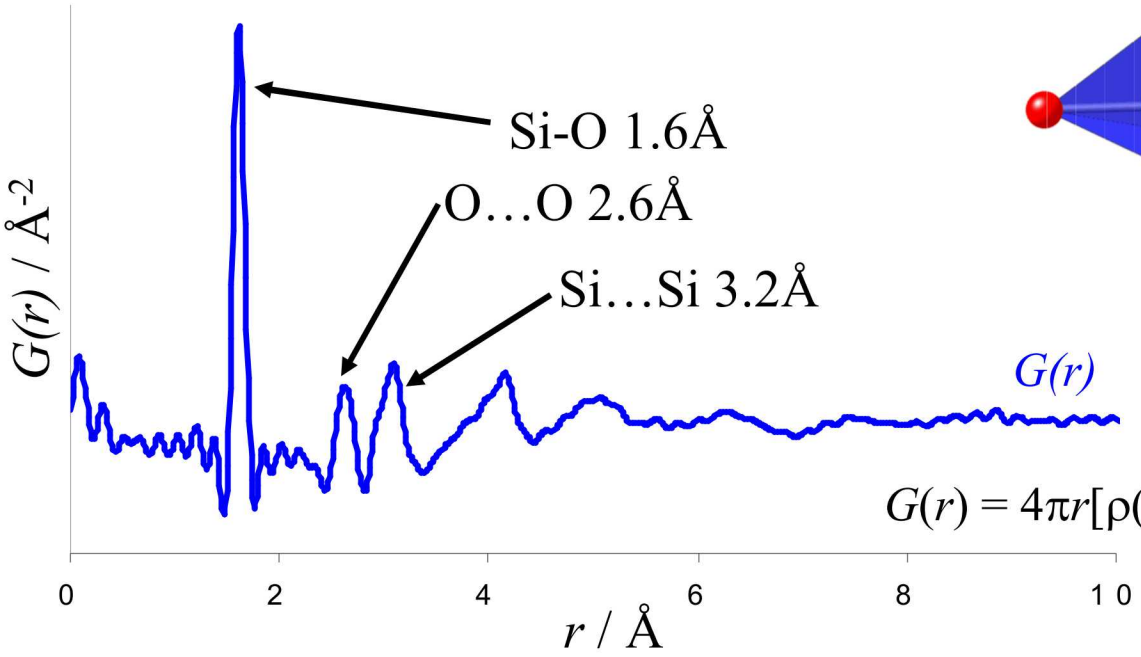


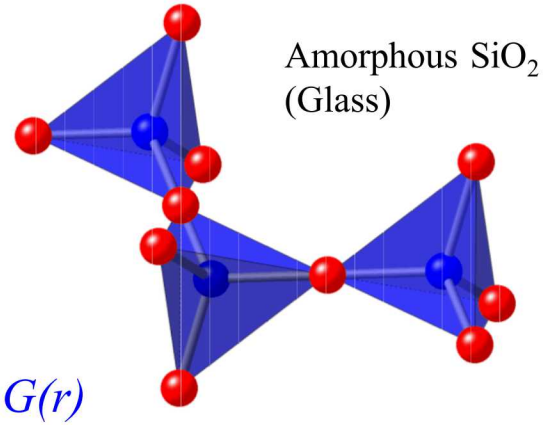


Peak position ⟷ Bond length / distance
Peak area ⟷ Coordination #, scattering intensity
Peak width ⟷ Disorder, bond angle distribution
Peak $r_{max}$ ⟷ Particle size, coherence

→ **Structural Modeling**

***Application to Zeolites to Examine Short Range Interactions of Guests in Pores***

# Applications

Reprocessing: capture on nonburnable volatile fission products and lesser actinides

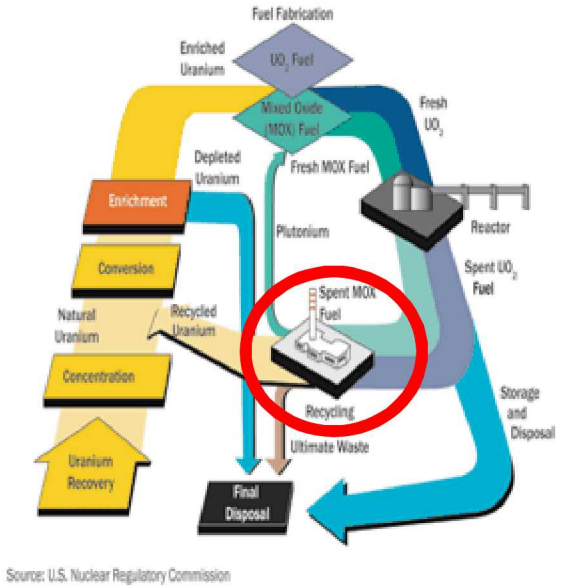


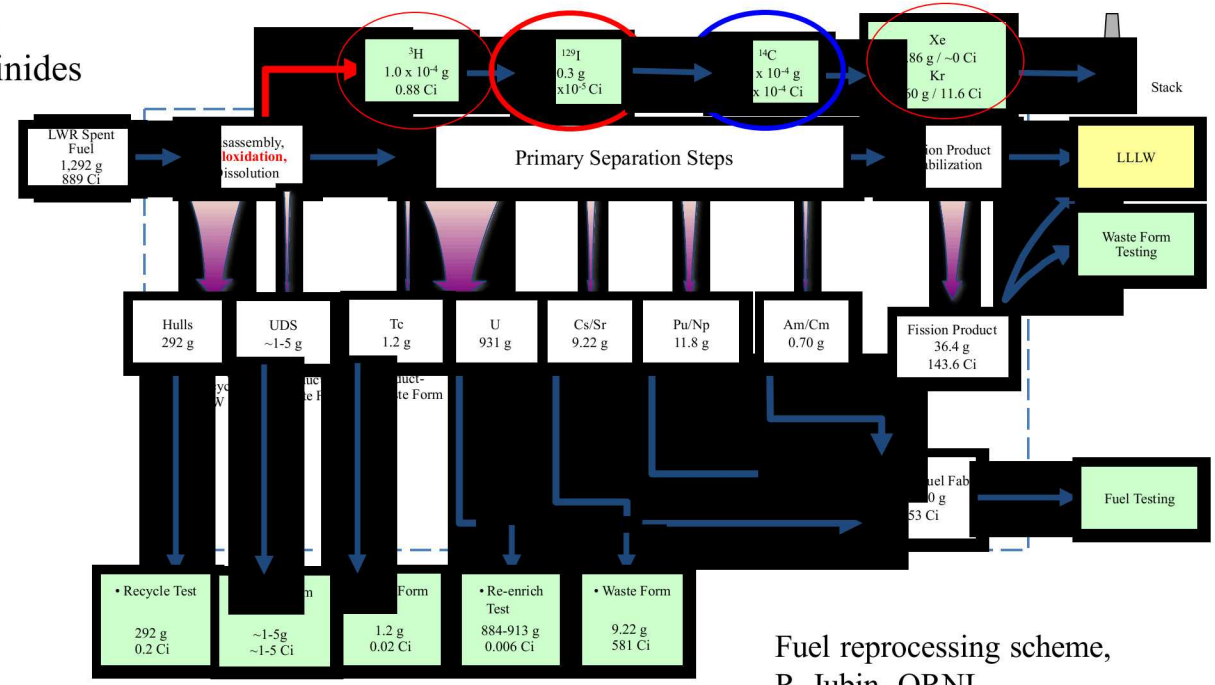


Fuel reprocessing scheme, R. Jubin, ORNL, FCRD-SWF-2011-000306

Legacy, Accident or Produced rad aqueous waste requiring highly specific ion capture

*Fukashima Daiichi* Nuclear Power Plant explosion 2011 $I^{129}$, $I^{131}$ volatile gas released; $Cs^{135}$, $Cs^{137}$ & $Sr^{90}$ aqueous released *(www.IAEA.org)*


# Outline

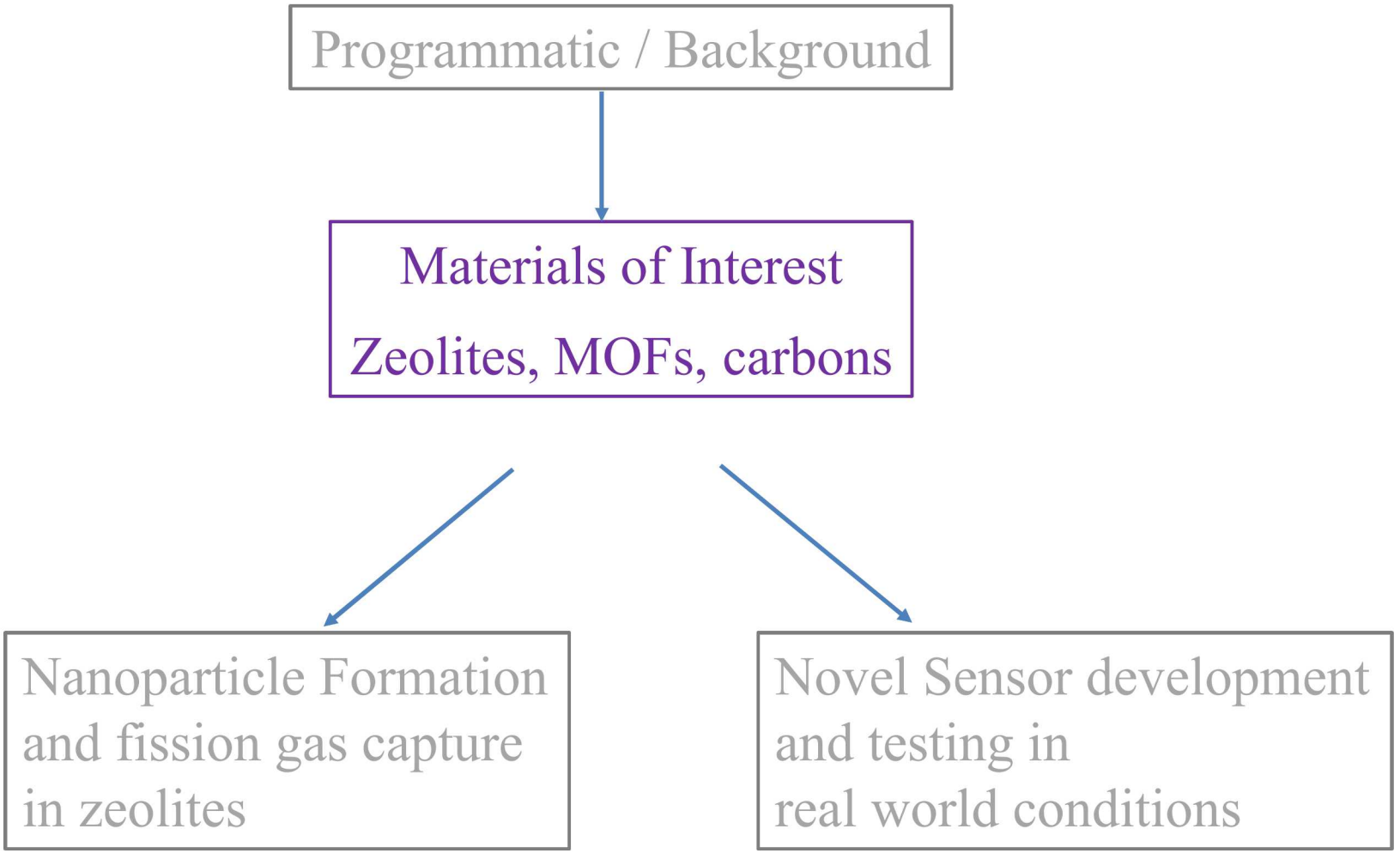
Programmatic / Background
Materials of Interest
Zeolites, MOFs, carbons
Nanoparticle Formation and fission gas capture in zeolites
Novel Sensor development and testing in real world conditions

# Ag-MOR zeolite, Traditional Iodine Capture Material

- While $I^{129}$ is only found in small concentrations in nuclear effluent, the effective capture and storage of iodine is critically important to public safety due to its involvement in human metabolic processes and its long half-life ($\sim 10^7$ years).

- Silver Mordenite (MOR) is a standard iodine-getter, although the iodine binding mechanism remains poorly defined. Presumably an iodide forms within the zeolite's pores

- Understanding **Structure-Property Relationship between Nanoscale and Bulk effects**
  - To optimize capture
  - Impacts processing for long term storage
  - To predict long term stability

MOR, Mordenite

$X_2Al_2Si_{10}O_{24}\bullet 7(H_2O)$

12 MR, 7.0 x 6.5Å

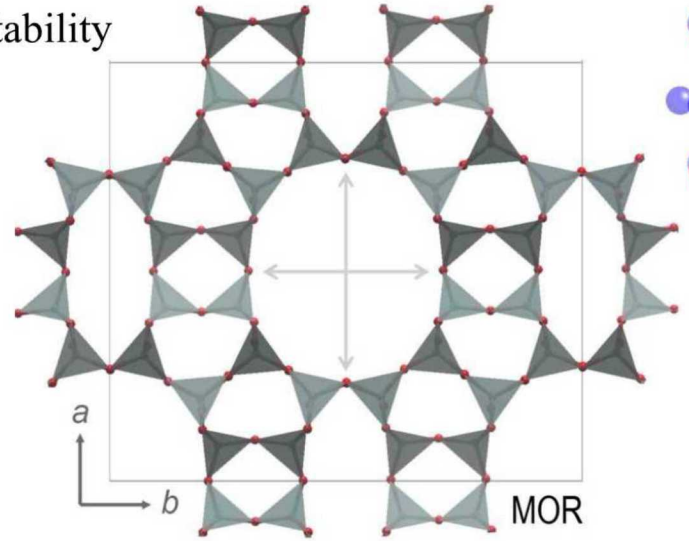


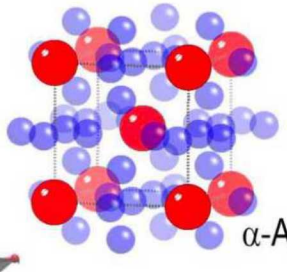


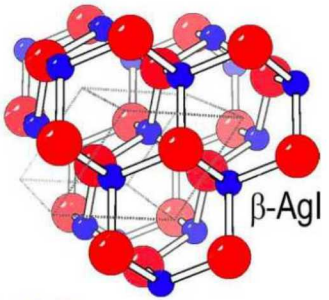


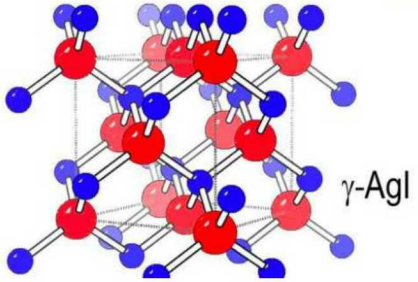

# Fundamental Studies of AgI-Zeolites: Ag-Mordenite (MOR) industry standard for $I_2$ capture

## Mordenite Topology and AgI Polymorphs

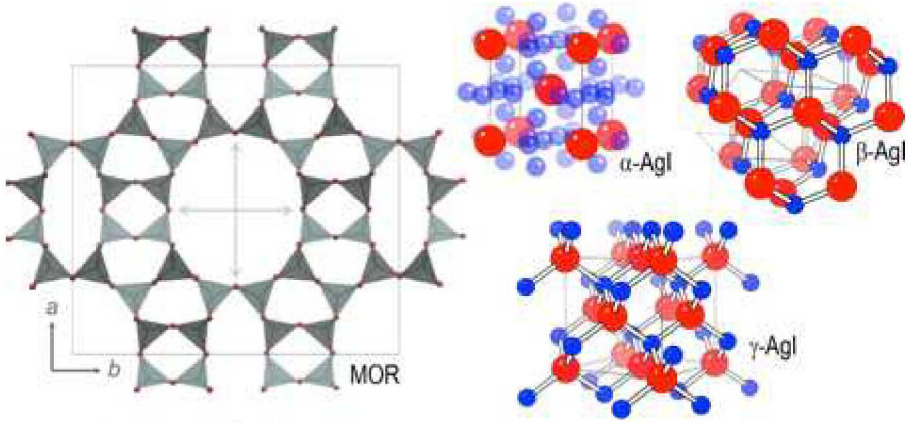


MOR, Mordenite

$X_2Al_2Si_{10}O_{24}\bullet 7(H_2O)$

12 MR, 7.0 x 6.5Å

Idealized MOR framework: *Used for Decades*

- 1D channels (12-rings, 6.5 x 7.6 Å) which contain exchangeable cations and water molecules (omitted).
- α, β, γ-AgI polymorphs (iodine-red; silver-blue)

MOR Samples from UOP: LZM5
$I_2$ gas exposure, saturated environment, 95°C
Ag reduction, 3% $H_2$ stream, 150°C

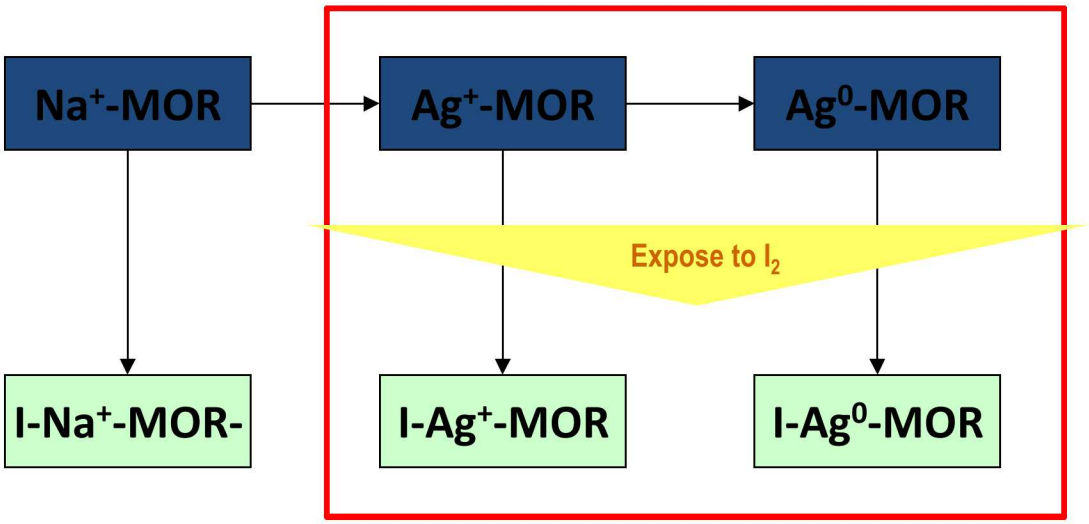


To study the capture of Iodine by either ion exchange or reduced Ag-MOR, samples were analyzed at ANL/APS by Pair Distribution Function (PDF) analysis

# *Differential*-PDFs: Fundamental Study of Zeolite Framework and Occluded AgI NPs

Synchrotron Pair Distribution Function Analysis (d-PDF) allows study of the AgI, minus the MOR zeolite framework (collaboration SNL & ANL/APS)

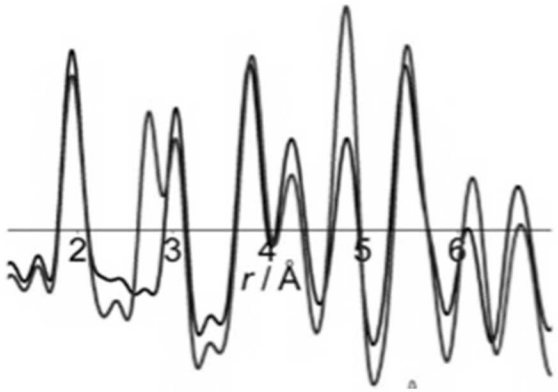


$G(r)_{Ag\text{-}I\text{-}MOR} - G(r)_{Ag\text{-}MOR}$

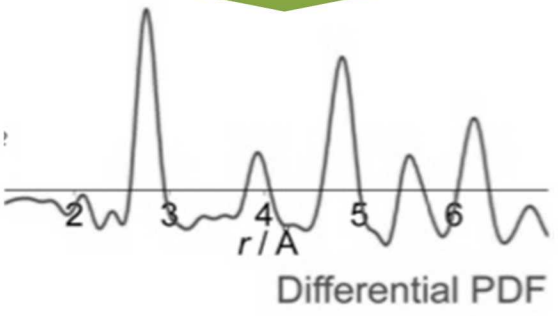


*In-zeolite pore capture*

| | Form | *r*-range (Å) | $R_{fit}$ | Phase Composition[§] | | | |
|---|---|---|---|---|---|---|---|
| | | | | $Ag^0$ | α-AgI | β-AgI | γ-AgI |
| $Ag^+$-I | on MOR | 2-10 | 27.5% | – | 1 | – | – |
| $Ag^0$-I | on MOR | 2-30 | 18.0% | – | 0.6 | – | 0.4 |
| AgI (Aldrich) | bulk | 2-30 | 13.6% | – | – | 0.53 | 0.47 |
| AgI ($Ag^0$+$I_2$) | bulk | 2-30 | 7.97% | 0.5 | – | – | 0.5 |
| $Ag^0$ | on MOR | 2-30 | 9.15% | 1 | – | – | – |

[§] $Ag^0$ (*Fm*-3*m*, $a = 4.08$ Å); α-AgI (*Im*-3*m*, $a = 5.0$ Å, $r < 7$ Å); β-AgI ($P6_3mc$, $a = 4.6$ Å, $c = 7.8$ Å, wurtzite structure); γ-AgI (*F*-43*m*, $a = 6.5$ Å, zinc blende structure).

# Mechanism Determined:
# State of the Ag determines I capture

Ag°-MOR + $I_2$ yields a mixture of γ-AgI bulk surface nanoparticles and sub-nanometer α-AgI.
$Ag^+$-MOR + $I_2$ produces exclusively sub-nanometer α-AgI ("**perfect fit**", confined in pores)

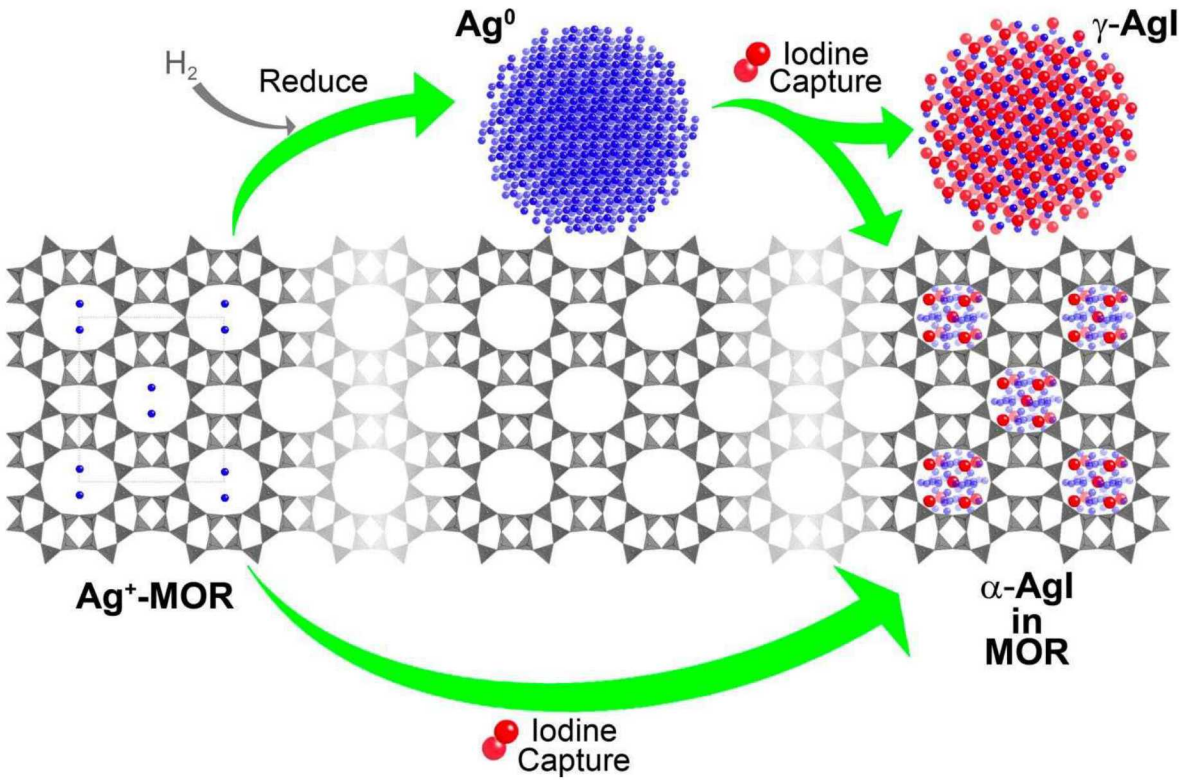


*JACS*, **2010**, *132* (26), 8897

*Issue associated with Zeolites do include the **need for Ag** and the difficulty of working with zeolites that **selectively adsorb $I_2$ and Org-I,** but **not $^3H_2O$, and Xe***

# AgI nanoparticle formation in MOR (from $Ag^+$-MOR + iodine species)

*JACS,* **2010**, *132*(26), 8897

*MMM,* **2014**, *200*, 297

## Ag-MOR + $I_2$

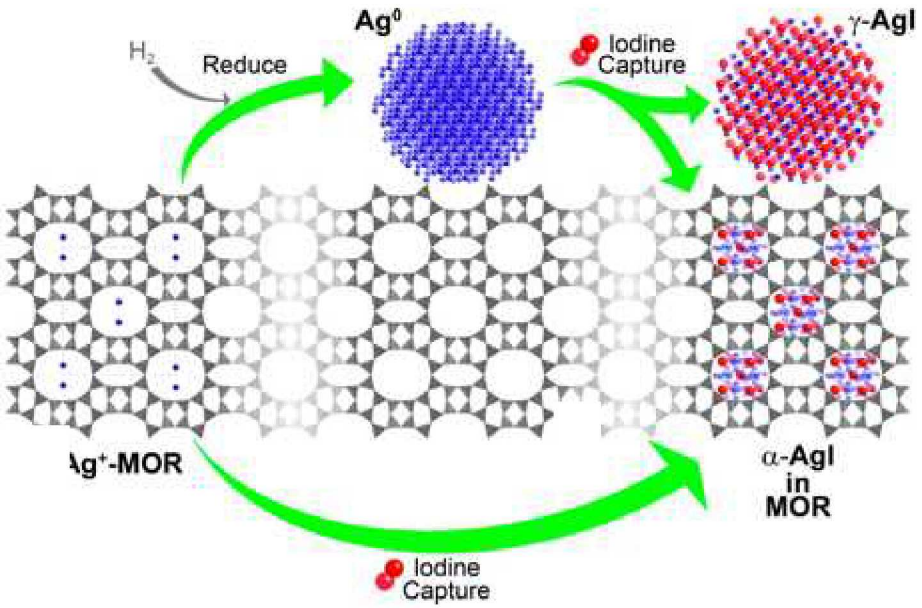


## Ag-MOR + $CH_3$-I

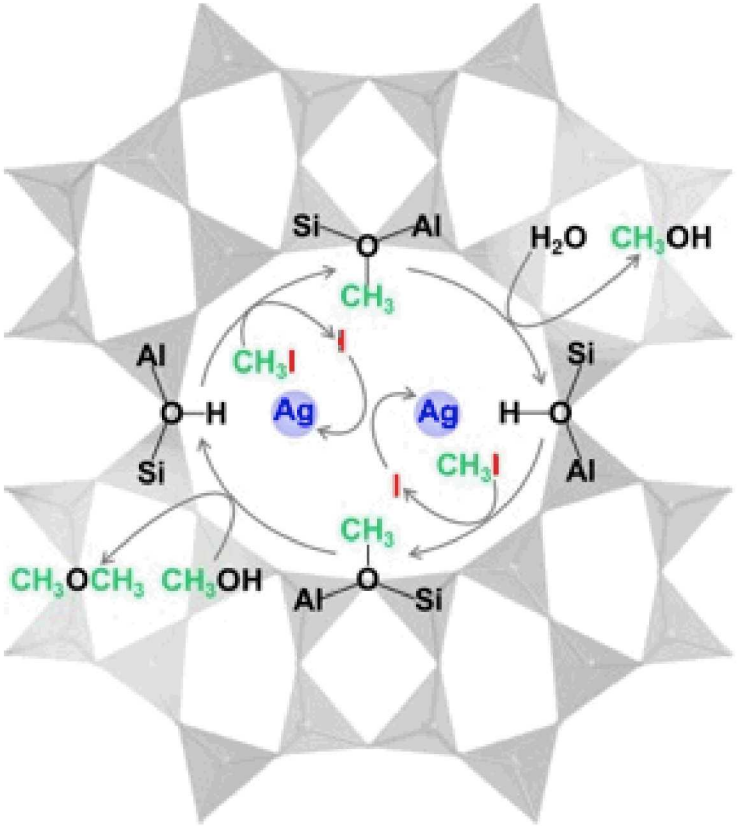


Mechanism of AgI formation & phase determination

# Metal Organic Frameworks (MOFs) for fission gas adsorption: iodine ($I_2$)

Traditionally zeolites/molecular sieves are used as baseline materials for selectivity and sorption. Cutting edge materials are tuned for high selectivity and high capacity.

Basolite Z1200, ZIF-8
Constricted Pore Opening (≈ 3.4Å)
1100 – 1600 $m^2/g$
Pore Volume = 0.636 cc/g
stable in Air & $H_2O$

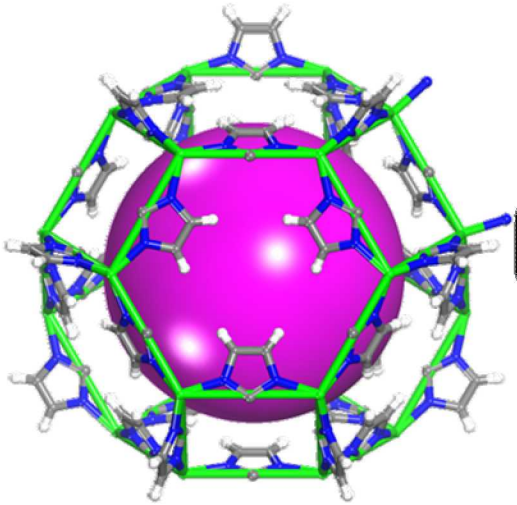

$I_2$@ZIF-8 ~ 125 wt.% $I_2$

*JACS*, **2011**, *133*(32),12398

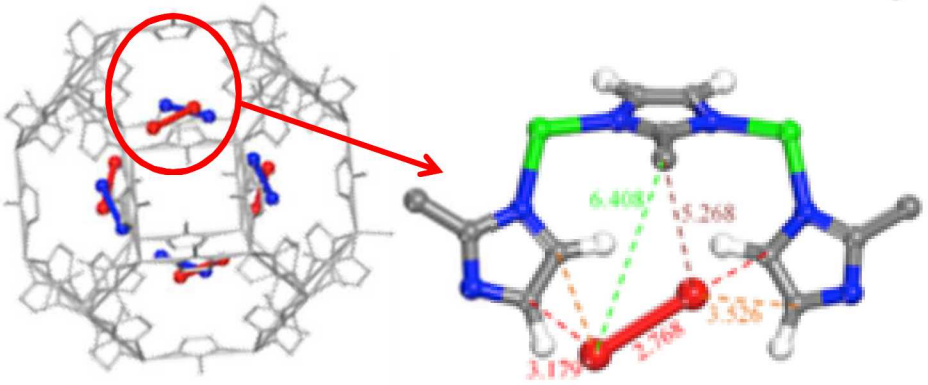


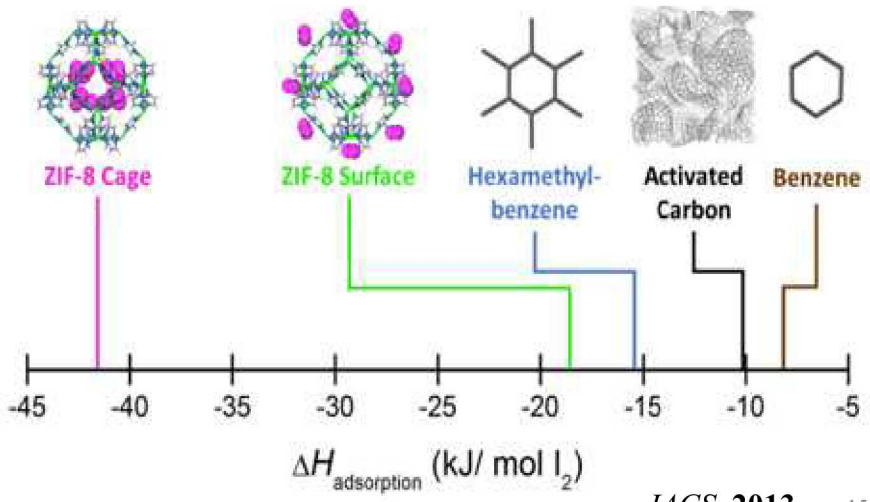


$I_2$ is selectively captured by ZIF-8 due to:
- *Size selectivity*
- *Iodine bound to organic ligand*

*JACS*, **2013**

# Crystal Structure of $I_2$@HKUST-1, selectivity of $I_2$ over $H_2O$

$I_2$/HKUST-1 **3.3 I/Cu**

Sava Gallis, Nenoff, et.al., *Chem. Mater.*, **2013**, *25* (13), 2591

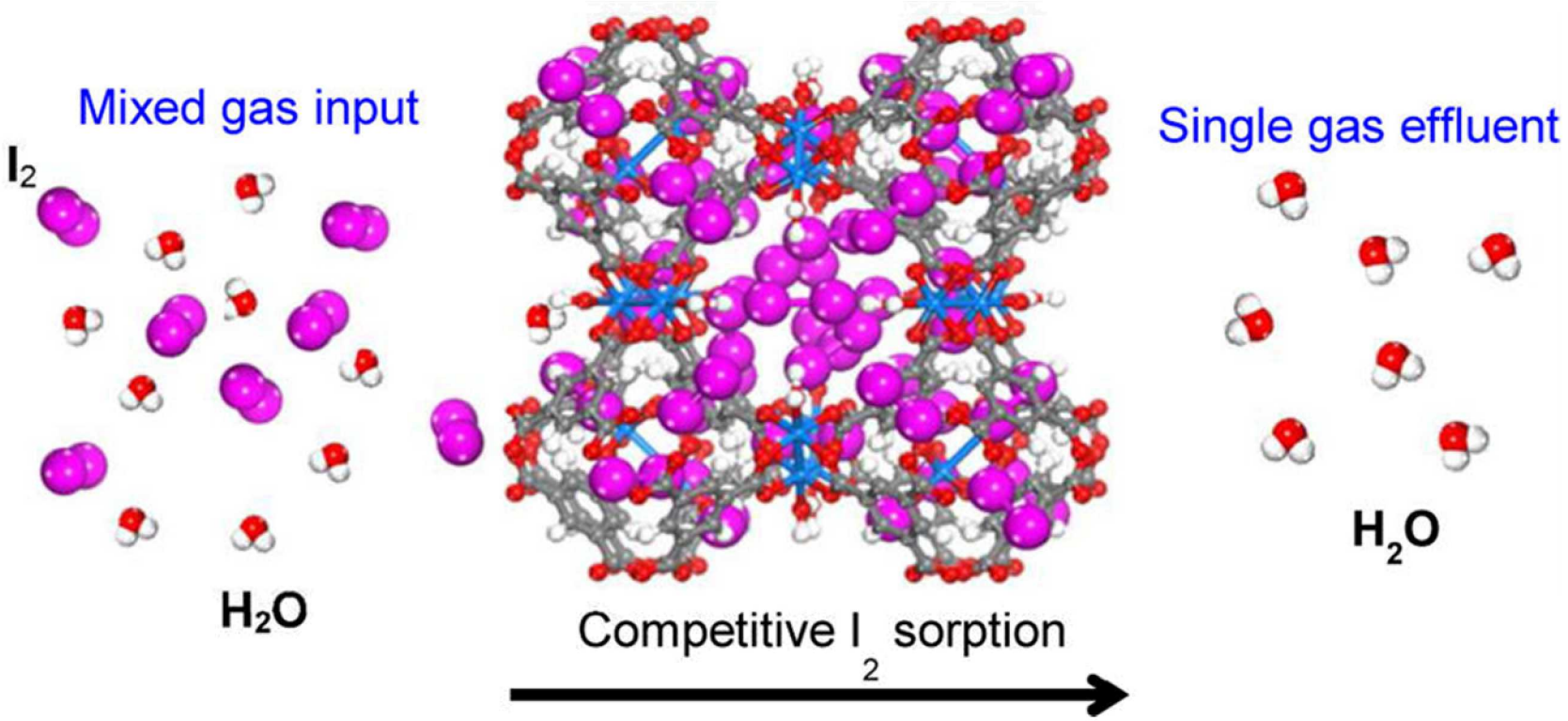


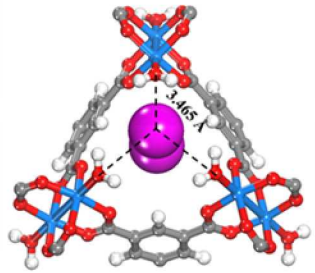


Iodine – Metal center (Cu) strongly bound
High Selectivity!
*Trumps* hydrophilicity of MOF

# Outline

Programmatic / Background

Materials of Interest

Zeolites, MOFs, carbons

Nanoparticle Formation and fission gas capture in zeolites

Novel Sensor development and testing in real world conditions

# Tunable Impedance Spectroscopy Sensors via Selective Nanoporous Materials

The ability to sense and identify *individual gases* from the complexity of the environment requires highly selective materials.

- Current conductivity-based devices generally fall into two categories:,
  - Solid state - (oxide based) require higher temperatures (>200°C) for interaction of the gas with the surface oxides; heating devices are needed.
  - Fuel cell – room temperature liquid electrolyte, easily fouled, short lifetime

- Utilization of *nanoporous metal organic frameworks (MOFs;* exceptionally high selectivity of gases of interest (eg., $I_2$) under ambient conditions) with *impedance spectroscopy* allows for novel sensing technologies

*Sensors*, **2009**, *9*, 1574

# Comparison studies of $I_2$ adsorption on Various Nanoporous Materials

Using a combination of Modeling (GCMC) and Iodine ($I_2$) Adsorption Studies to compare various nanoporous phases for iodine adsorption

MOFs, Zeolites/Molecular Sieves, Activated Carbons/Charcoals:

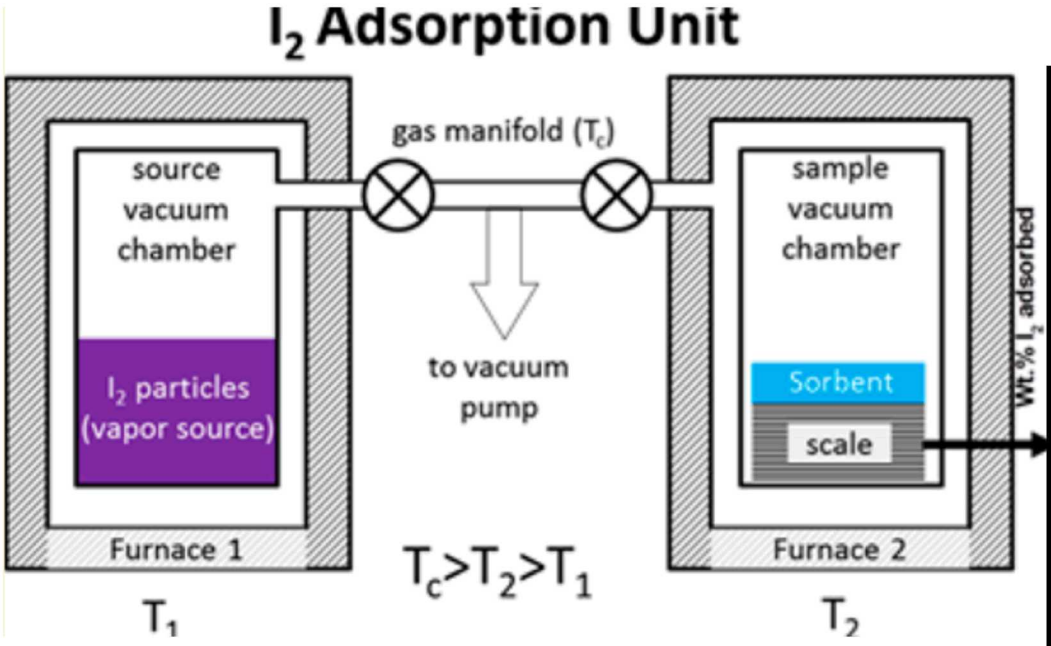


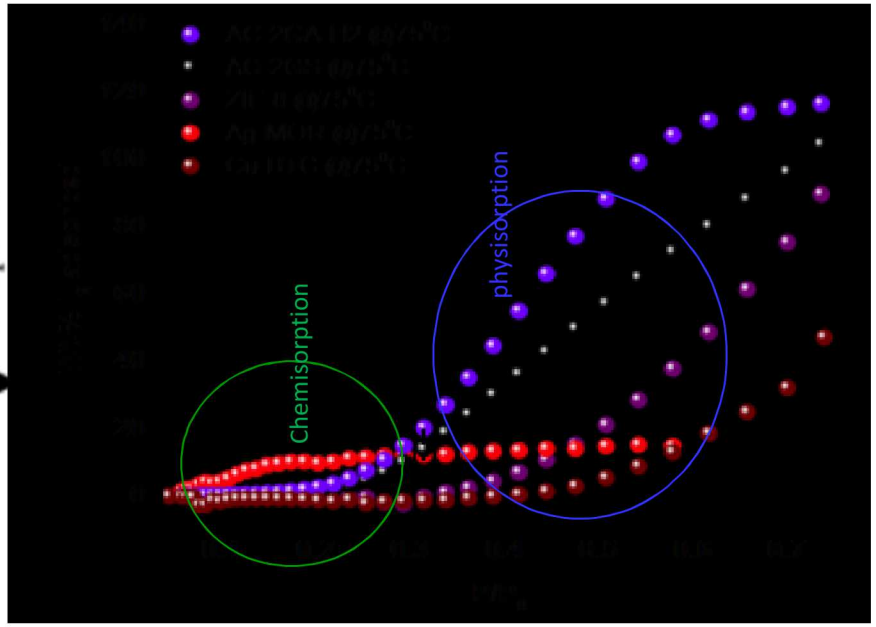


**$P/P_o$ <0.3: $I_2$** adsorption occurs in **small pores** & **strong chemisorption interactions** with framework or extra framework

*Ind. Eng. Chem. Res.*, **2017**, 56(8), 2331

# $I_2$@MOFs Sensors, to date…

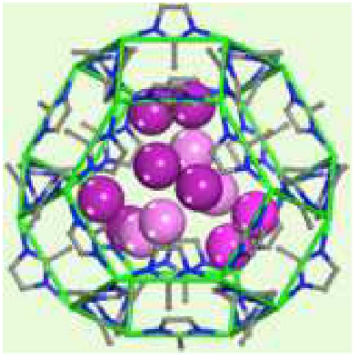

$I_2$@ZIF-8

*JACS* **2011**, *133* (32), 12398

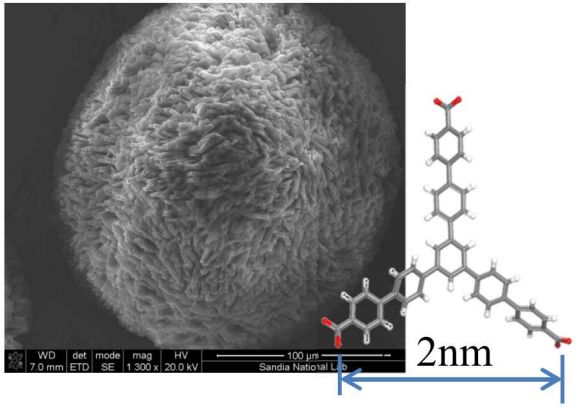


$I_2$@SMOF-3

*Chem. Mater.* **2014**, *26* (9), 2943

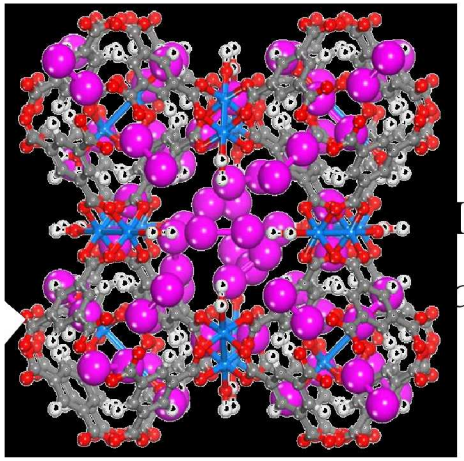

$I_2$@HKUST-1

*Chem. Mater.*, **2013**, *25* (13), 2591

$I_2$@AC

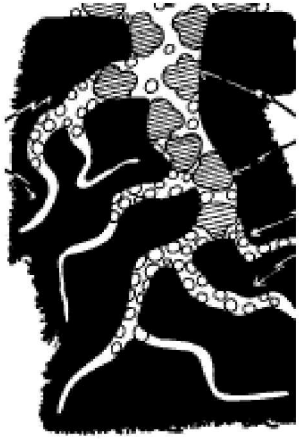

- $I_2$ has a low vapor pressure and is highly polarizable, once adsorbed into MOF
- Screen printed onto patterned array of IDE
- Impedance spectra measured ***in real time*** as the MOF is exposed to gas vapor at varying temperatures to **tune responses**.

# Iodine Sensors with High Selectivity in Environmental Conditions

**Impedance spectroscopy,**

polarizable molecules increase the capacitance and thereby decrease the impedance.

The selectivity of MOFs for $I_2$ under mild conditions paired with the **polarizability of the $I_2$** molecules, enables real-time electrical sensing (direct electrical readout) via impedance spectroscopy.

Common air component gas molecules such as Ar, $O_2$ and $N_2$ are not/not-highly polarizable molecules

**Modular platform:**

able to test MOFs of different configurations, metal centers and charge transfer capabilities

*Real-Time sensing by impedance spectroscopy (IS):*

All measurements to date are simple single sine measurements.

The electrical test equipment generates a single sine voltage wave at a given frequency,

& measures the returned current in terms of its:

- **magnitude** (this relates to the impedance, |Z| on the plots) and
- **phase angle** compared to the original voltage wave

In fast fourier transform (FFT), a voltage pulse is sent out.

The pulse is the FFT of 20+ frequencies.

The measurement time is limited by the lowest frequency.

High Efficient Method: can collect ~ 20 data points in nearly the same time as the 1 lowest frequency data point.

This is all contained in commercial equipment and software.

# Iodine Sensors with High Selectivity in Environmental Conditions

Solartron 1296 dielectric interface in series with a Solartron 1260 frequency response analyzer.
All sensor testing in a faraday cage to minimize electrical noise.

Samples are contacted with tungsten probes.

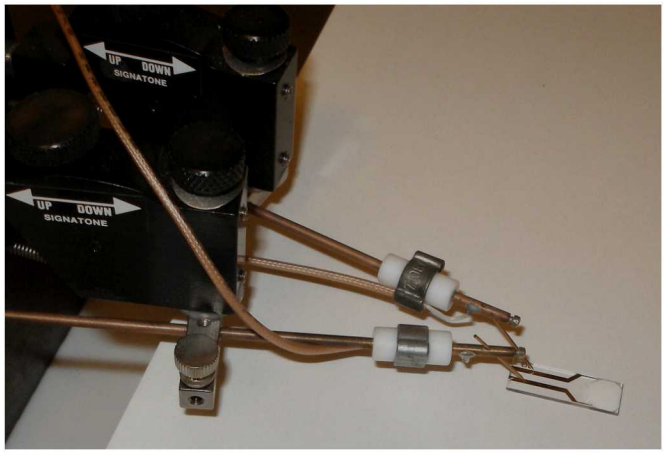


The dielectric interface allows us to **measure impedances as large as $10^{14}$ Ohms and frequencies 1 mHz – 1 MHz.**
**Unique SNL specific: specialized high impedance, low frequency test equipment**
(Common electrical test equipment has a lower input impedance than these coatings)

- Inter Digitated Electrodes (IDE's):
  10 μm wide platinum lines (125 pairs), 10 μm spacing on glass substrate
- MOF film: MOF + binder
- Film: screen printed onto platinum interdigitated electrodes
- Iodine adsorption studies: in air and humidity at 25, 40, 70 ˚C
- Test response over a broad electrical frequency response (1 MHz – 1 mHz)

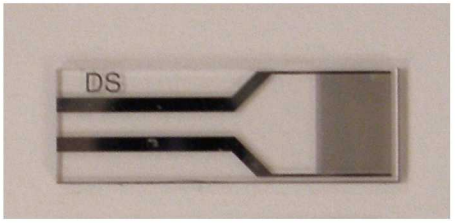

# $I_2$@Nanoporous Materials Sensors, to date…

## MOR zeolite

*JACS*, 2010, 132(26), 8897

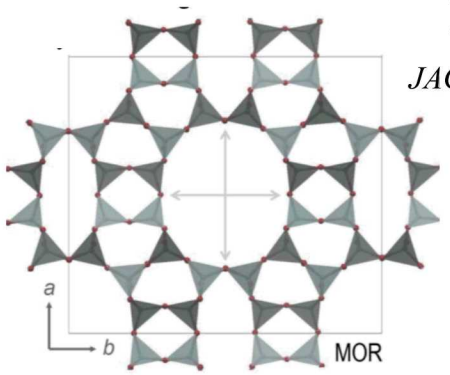


## $I_2$@SMOF-3

*Chem. Mater.* **2014**, *26* (9), 2943

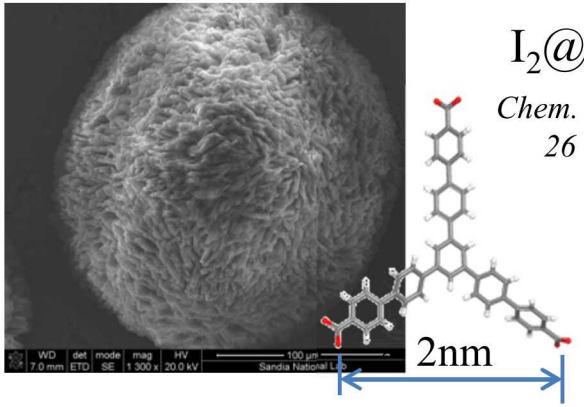


## $I_2$@HKUST-1

*Chem. Mater.*, **2013**, *25* (13), 2591

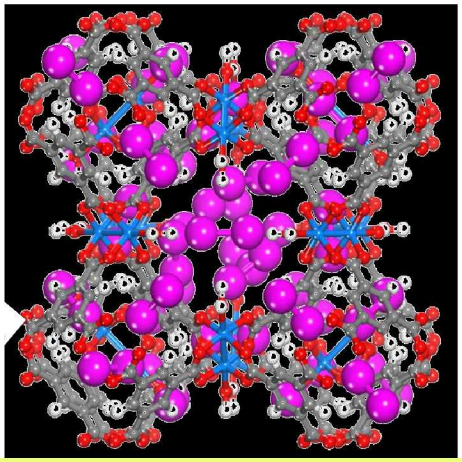

## $I_2$@ZIF-8

*JACS* **2011**, *133* (32), 12398

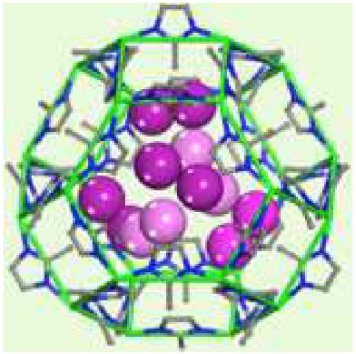

## $I_2$@AC

*I&ECR.*, **2017**, 56(8), 2331

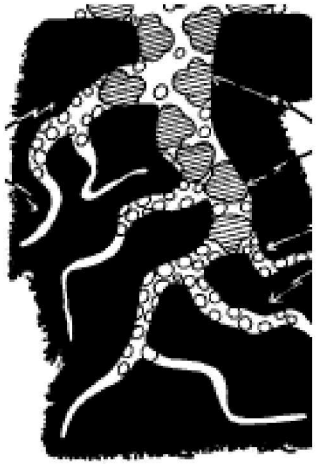

- $I_2$ has a low vapor pressure and is highly polarizable, once adsorbed into MOF
- Screen printed onto patterned array of IDE
- Impedance spectra measured ***in real time*** as the MOF is exposed to gas vapor at varying temperatures to **tune responses**.

# Electrical Readout Effect of Ag-MOR zeolite when exposed to $I_2$

Dropcast 2 x 25 µL of mordenite in $CH_3Cl$ (100mg/1mL)
Dry 70 °C for 30 min in air
Exposed to $I_2$ at 70 °C for 30 min
"Dry" 70 °C for 30 min in air

All mordenite is LZM-5 quality, ion exchanged + reduced at Sandia.

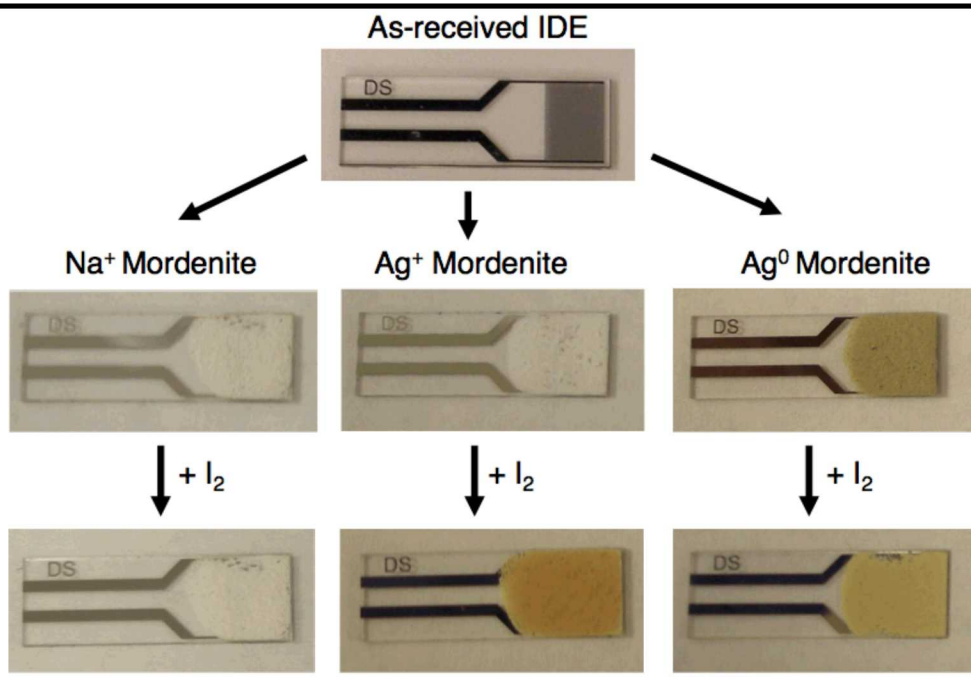


| Mordenite Type | Mordenite Deposited / mg | $I_2$ Sorbed / % of Mordenite mass | # of samples |
|---|---|---|---|
| $Na^+$ | 4.76 ± 0.59 | -1.1% ± 0.6% | 3 |
| $Ag^+$ | 3.74 ± 0.32 | 11.6% ± 1.1% | 4 |
| $Ag^0$ | 3.23 ± 0.26 | 9.7% ± 1.6% | 4 |

* Reproducibility in film thicknesses and therefore iodine adsorption

Small & Nenoff, **2018**, in prep.

# *Electrical Readout Data* is dictated by final iodine capture mechanism

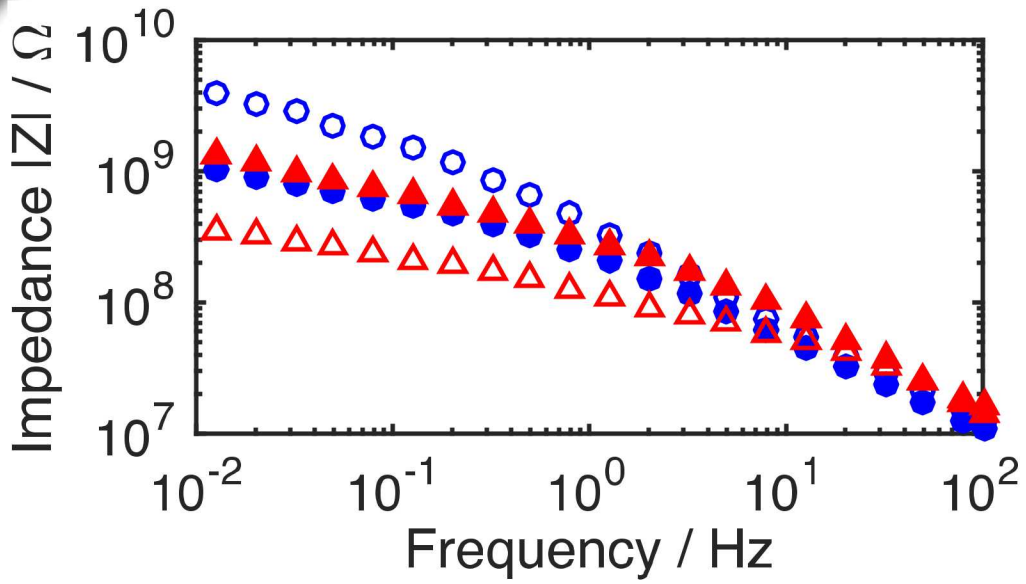


- $Ag^+$ Mordenite
- $Ag^+$ Mordenite + $I_2$
- $Ag^0$ Mordenite
- $Ag^0$ Mordenite + $I_2$

Impedance responses of $Ag^+$-Mordenite and $Ag^0$-Mordenite: ***converge upon iodine sorption***

Ag-MOR + $I_2$ → AgI-MOR

Impedance response data seems to have a direct correlation to the formation of the AgI nanoparticle (ionic)

- $Ag^0$ increases as $I_2$ is adsorbed. (conductor to modest conductor)
- $Ag^+$ decreases in impedance as $I_2$ is adsorbed (insulator to modest conductor)

**Final result independent of starting Ag ionic state in the zeolite**

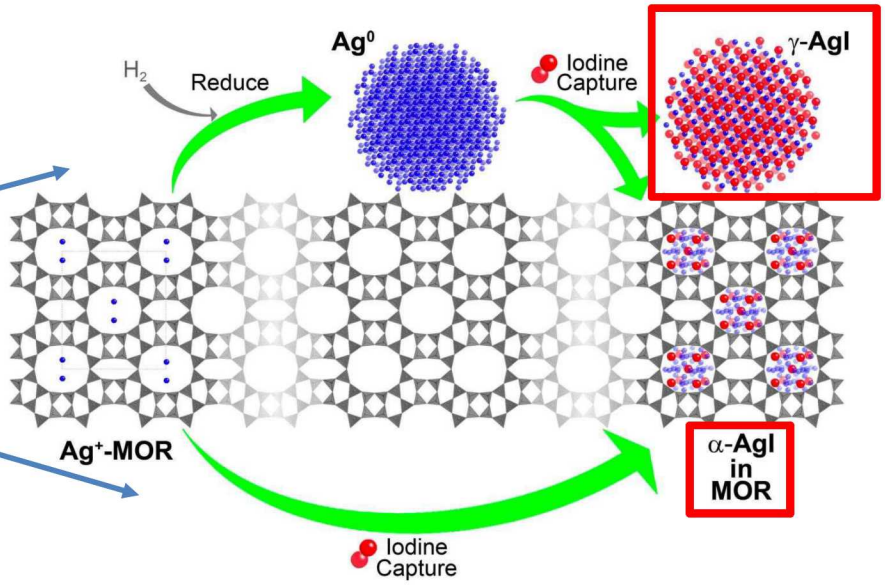

# *Electrical Readout Data* is dictated by final iodine capture mechanism

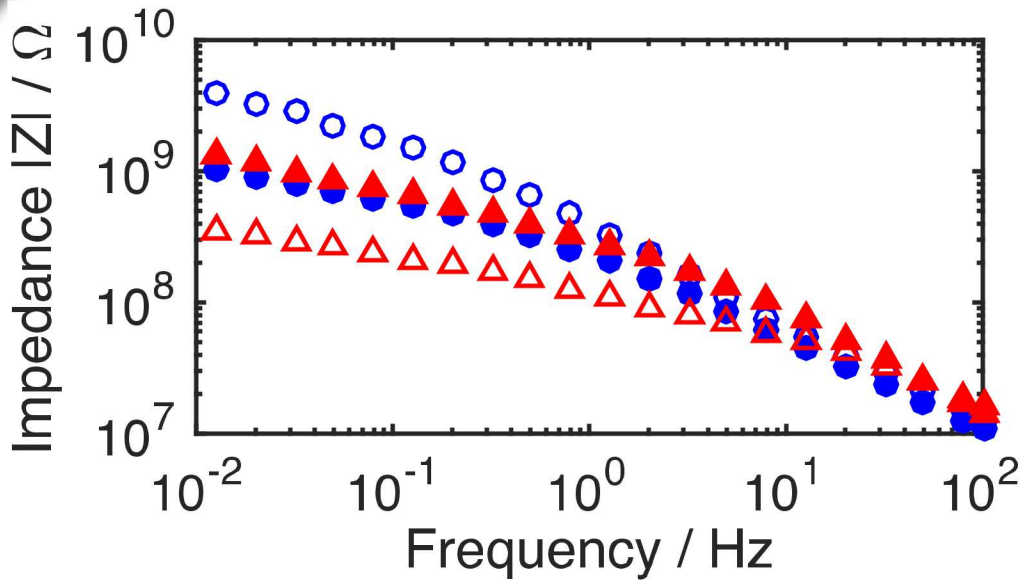


- $Ag^+$ Mordenite
- $Ag^+$ Mordenite + $I_2$
- $Ag^0$ Mordenite
- $Ag^0$ Mordenite + $I_2$

Impedance responses of $Ag^+$-Mordenite and $Ag^0$-Mordenite: ***converge upon iodine sorption***

A study of the phase angle response vs. frequency indicates there are *two different mechanisms* or charge transfer pathways here

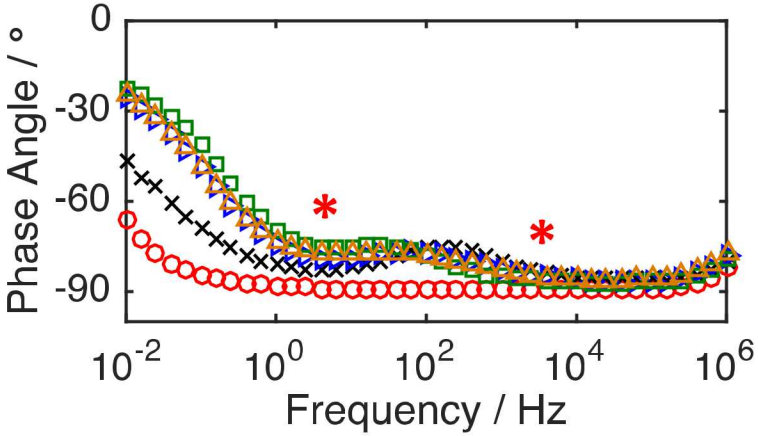


- IDE
- IDE + $Ag^+$ Mor
- IDE + $Ag^+$ Mordenite + $I_2$
- IDE + $Ag^0$ Mor
- IDE + $Ag^0$ Mor + $I_2$

# Modeling Charge Transfer Pathways in Ag-MOR

*diffusion-controlled movement of ions in porous films*

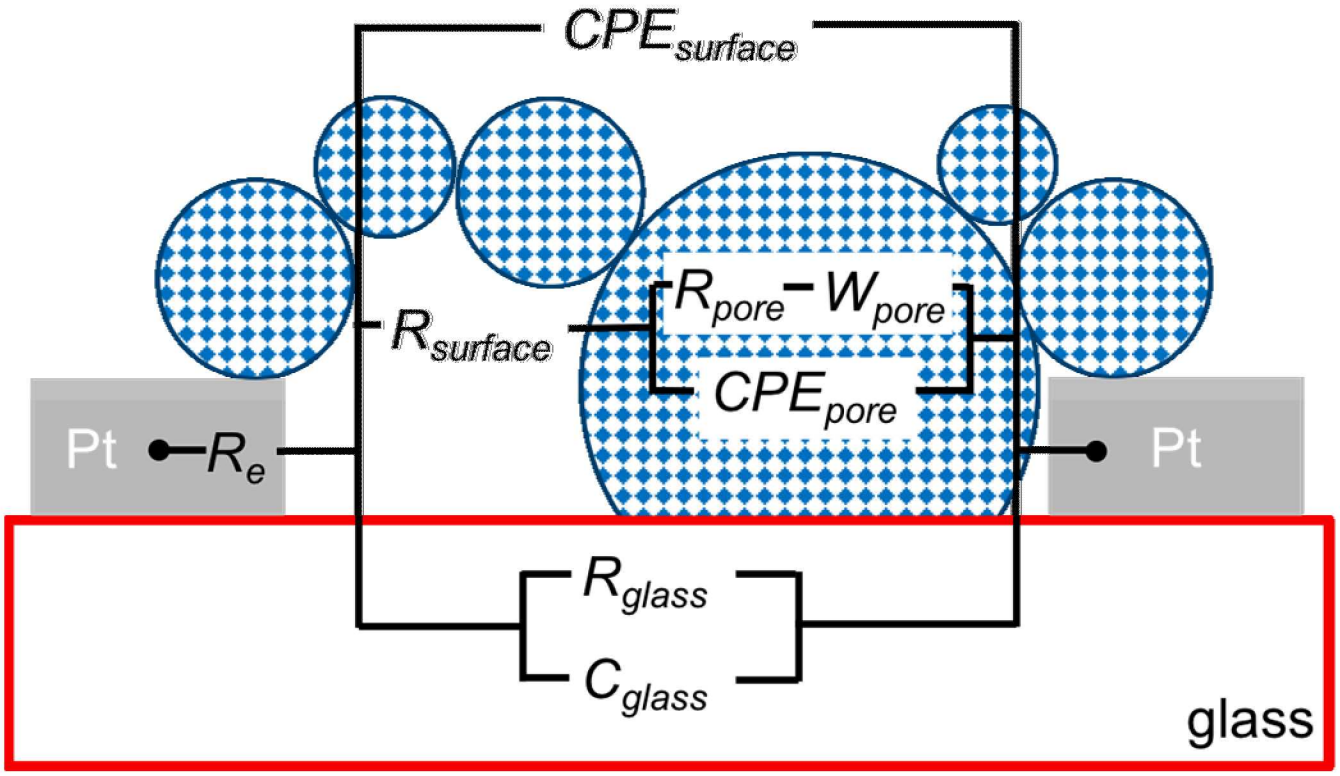


- Both the surface and pore interior offer charge transfer pathways.
- Must travel along surface before moving through a pore.
- Impedance of each pathway controlled by initial state ($Ag^{+}/Ag^{\circ}$) and $I_2$ loading.

# Effect of $I_2$ Exposure on Charge Transfer Pathways in Ag-Mordenite

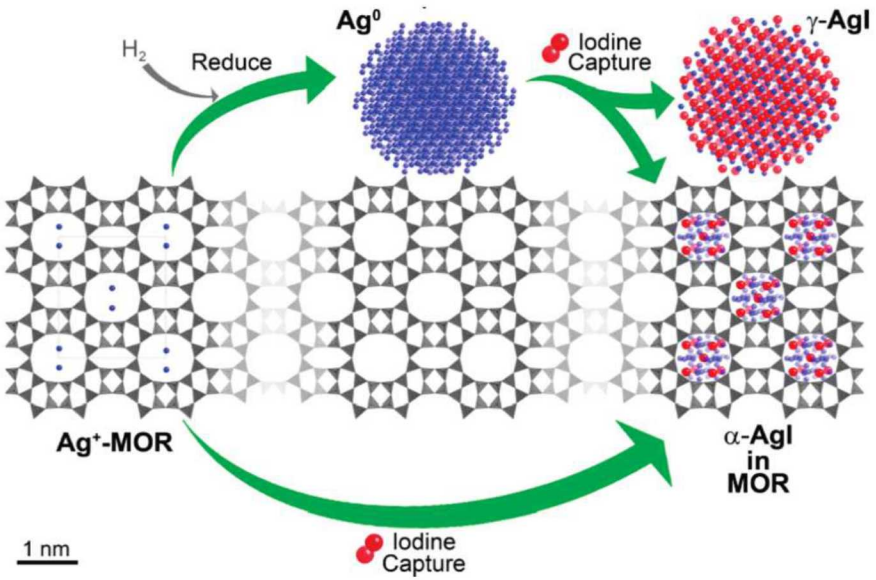


Chapman, Chupas, Nenoff, *J. Amer. Chem. Soc.*, **2010**,*132*, 8897.

Values fit using model

| | Change in Resistance after $I_2$ exposure | |
|---|---|---|
| | $R_{surface}$ | $R_{pore}$ |
| $Ag^0$ | +42.5% | -28.8% |
| $Ag^+$ | +65.8% | -42.5% |

$I_2$ exposure for 30 min at 70 °C

- $Ag^0$-Mor + $I_2$:
  - surface resistance increases as $Ag^0$ forms γ-AgI
  - pore resistance decreases as "empty" (protonated, $H^+$) pore forms α-AgI
- $Ag^+$-Mor + $I_2$:
  - surface resistance increases
  - pore resistance decreases as $Ag^+$ forms α-AgI

# Possible Mechanisms of Conductivity
## Two different routes: Internal Pores Only vs. Mixed Route

*Impedance Spectroscopy* is a measurement of both the **micro-** and **mesoscopic** properties of the films

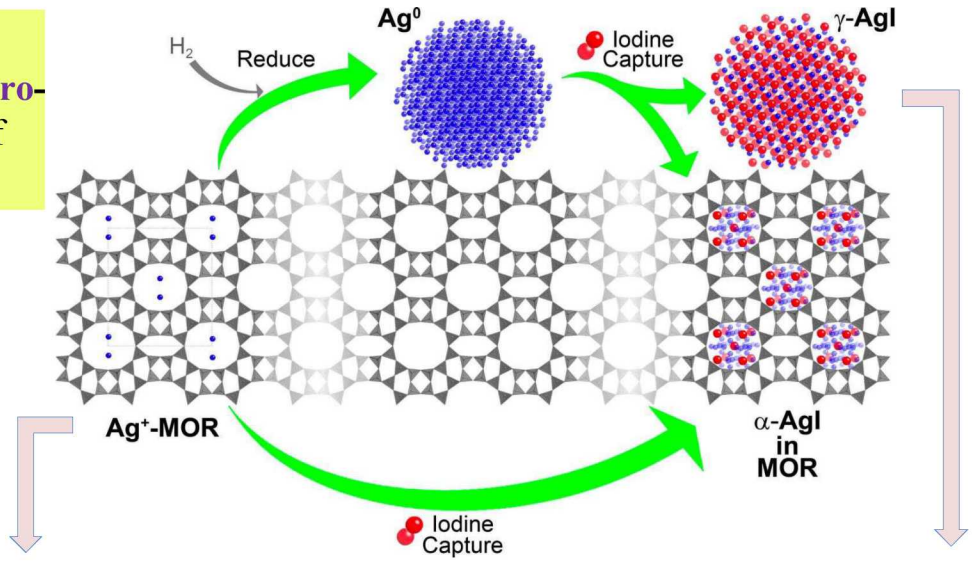


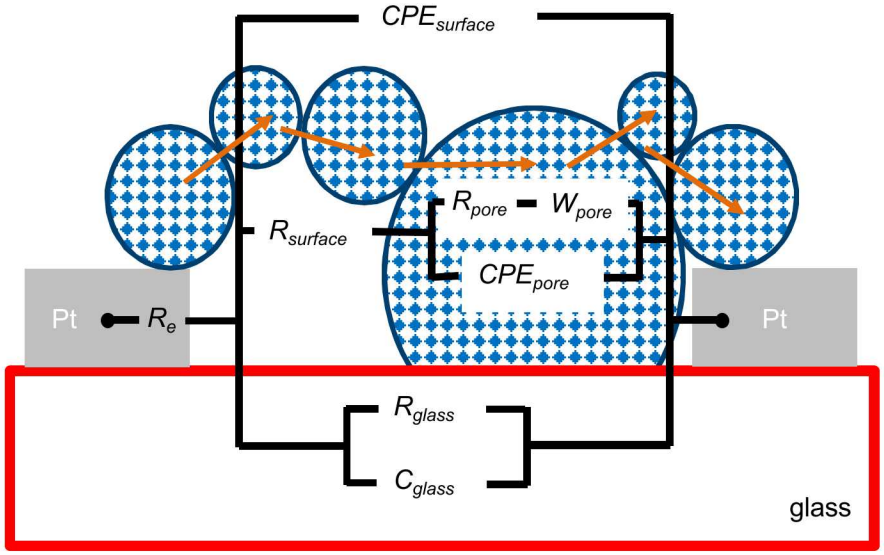


Ag⁺-MOR decreases in impedance as $I_2$ is adsorbed (insulator to modest conductor)

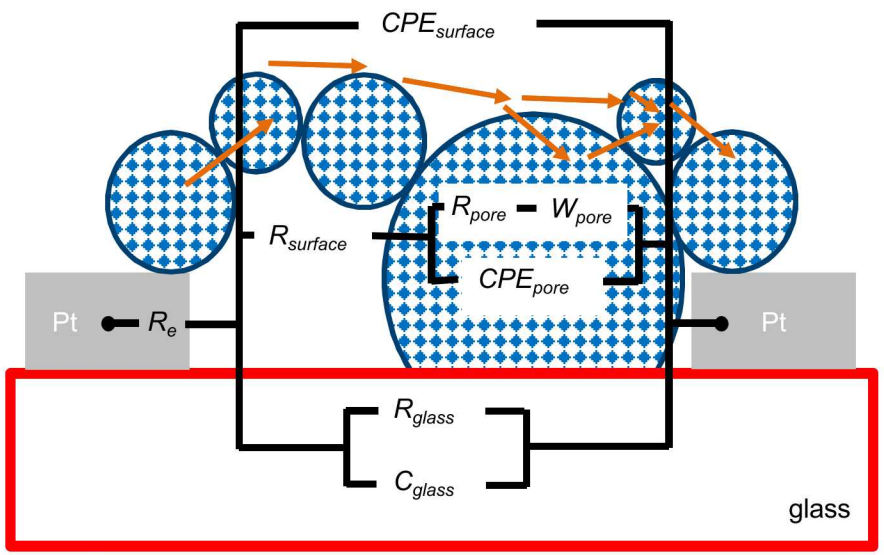


Ag⁰–MOR increases in impedance as $I_2$ is adsorbed (conductor to modest conductor)

# $I_2$@Nanoporous Materials Sensors, to date…

## MOR zeolite

*JACS*, 2010, 132(26), 8897

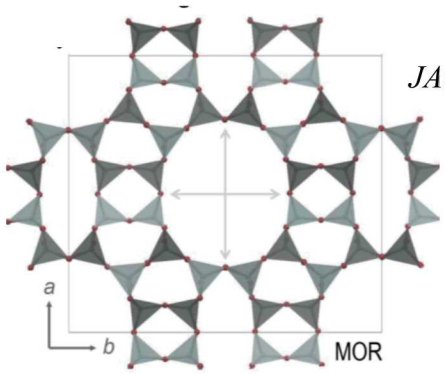


## $I_2$@SMOF-3

*Chem. Mater.* **2014**, *26* (9), 2943

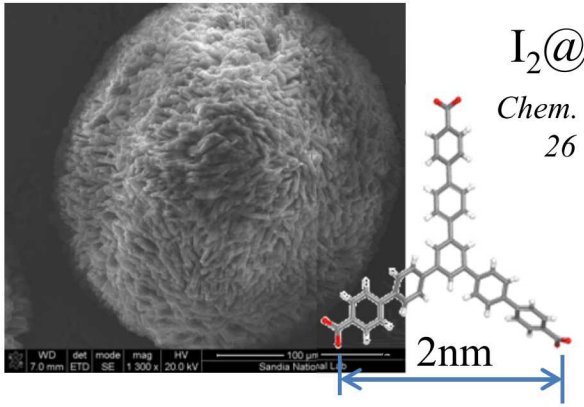


## $I_2$@ZIF-8

*JACS* **2011**, *133* (32), 12398

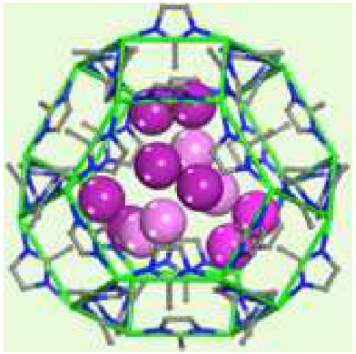

## $I_2$@HKUST-1

*Chem. Mater.*, **2013**, *25* (13), 2591

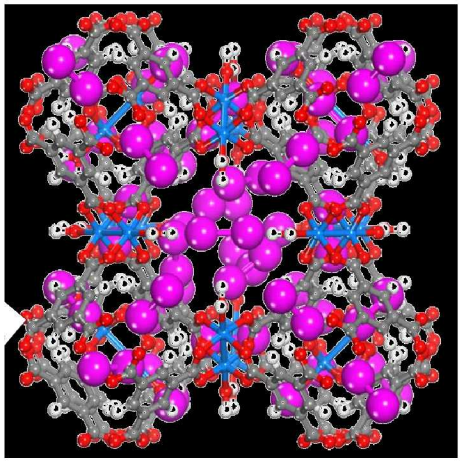

## $I_2$@AC

*I&ECR.*, **2017**, 56(8), 2331

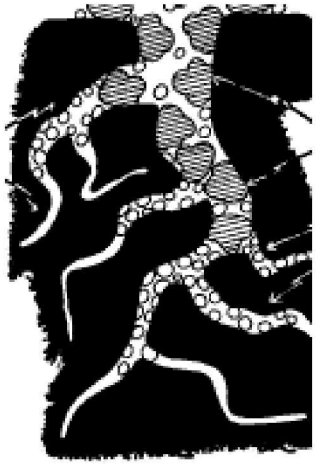

- $I_2$ has a low vapor pressure and is highly polarizable, once adsorbed into MOF
- Screen printed onto patterned array of IDE
- Impedance spectra measured ***in real time*** as the MOF is exposed to gas vapor at varying temperatures to **tune responses**.

# Iodine ($I_2$) Sensor with ZIF-8

as-received

ZIF-8

ZIF-8 + $I_2$ 70 °C

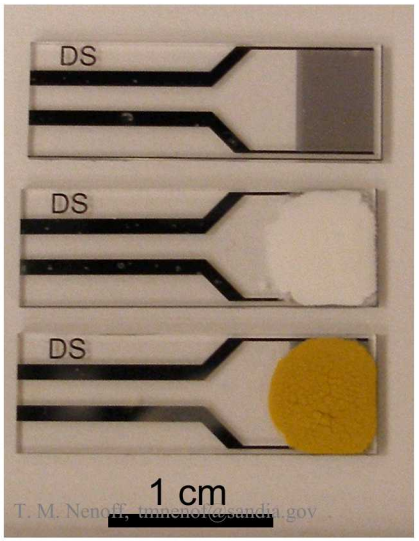


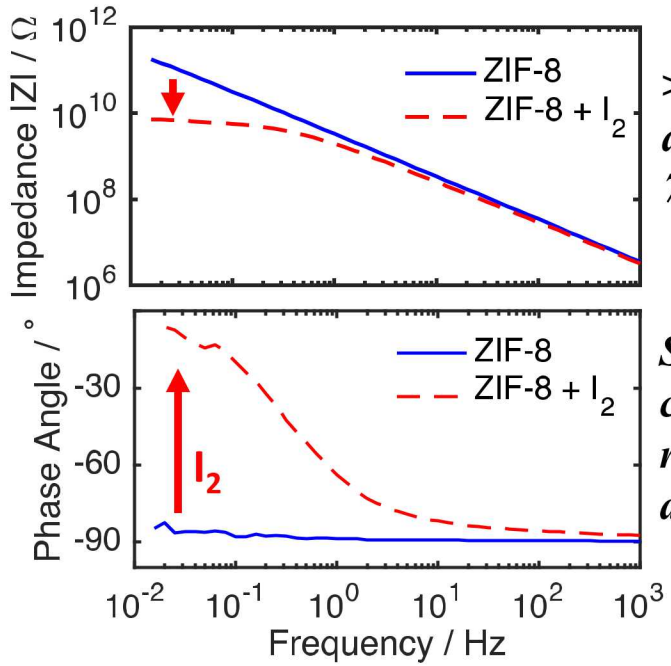


***>1 order magnitude decrease in impedance 70 °C, 30 min $I_2$ exposure***

***Sensor changes from ideal capacitor to nearly ideal resistor at low frequency after $I_2$ sorption.***

| Loading Temperature (˚C) | "Empty MOF" Device impedance (GΩ) | "$I_2$-Loaded MOF" Device impedance (GΩ) | % Change |
|---|---|---|---|
| Room temp. | 171 | 121 | -29% |
| 40 | 182 | 20.7 | -89% |
| 70 | 182 | 7.22 | -96% |

|Z| recorded at 15 mHz. 10 mV AC. 0 V DC.

*ACS Applied Mater. Interfaces*, **2017**, *9*, 44649

# Conclusion

Fission Gas selectivity is highly dependent upon local nanoscale interactions

Iodine species ($I_2$, Org-I)
Noble gases (Xe)
Tritium ($3H_2O$)

Use of **impedance spectroscopy (IS)** enables direct electrical readout of iodine gas presence, in ambient conditions of temperature and humidity
this is due to the *highly polarizable nature of* $I_2$

Enabled technology by both the nanoporous material and the gas molecules targeted.

Success with Impedance Spectroscopy (IS)
is ensured due to the ability to test 100 kHz – 1 Hz in 10 s using FFT methods

On-going research in sensors:
- off-gasing organic systems, organic-acids and other environmental gases of interest
- added durability by film application and protective capping components

# Outline

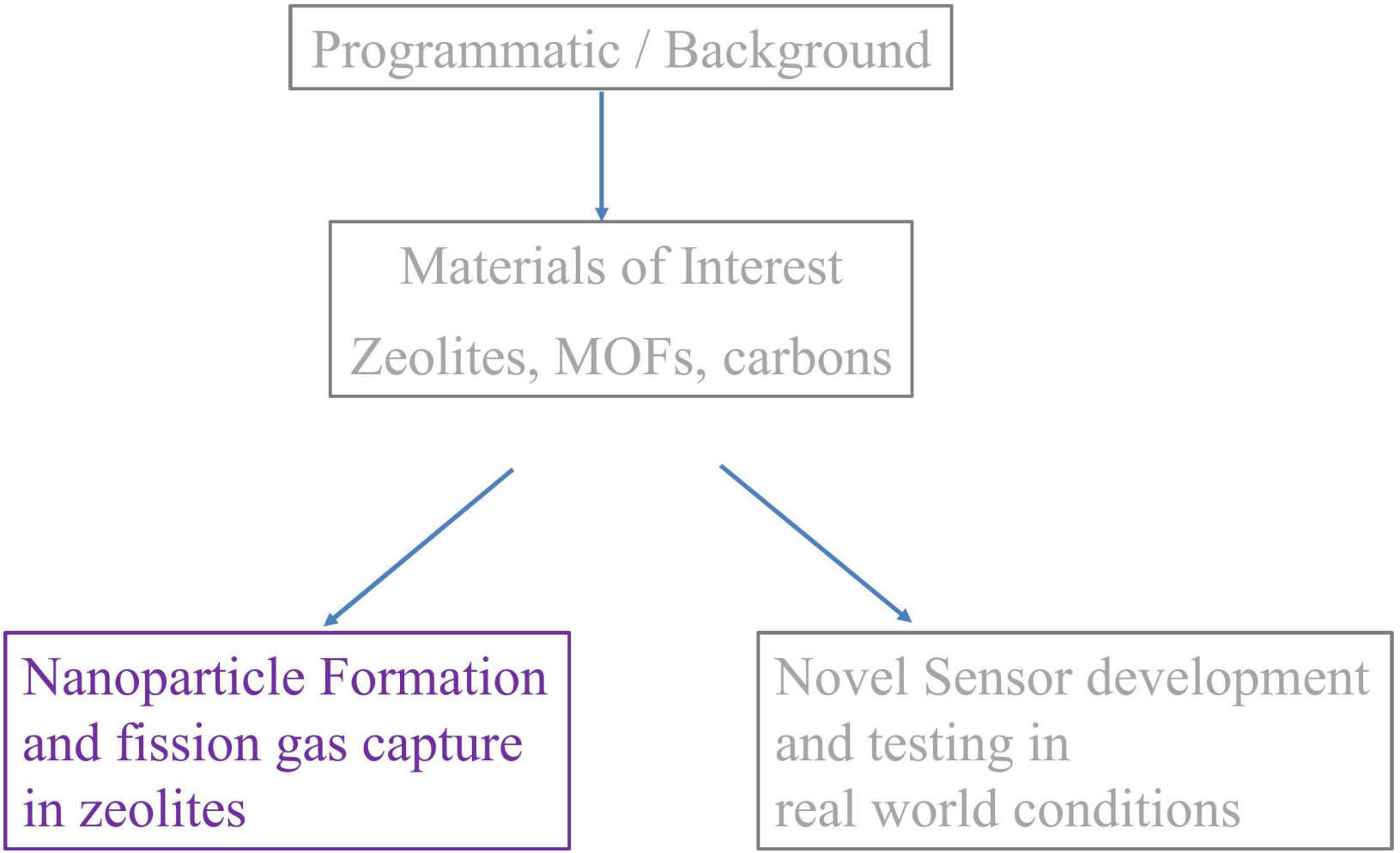
Programmatic / Background
Materials of Interest
Zeolites, MOFs, carbons
Nanoparticle Formation and fission gas capture in zeolites
Novel Sensor development and testing in real world conditions

# Nanoparticles in Nanopores

*Controlling the size and shape of nanoparticles is key to controlling their functional behavior*

Functionality can deviate significantly from bulk materials properties
such as in optical, electronic and catalytic behaviors

Bulk Silver is unreactive. However nanoscale silver particles exhibit valuable activities including
$NO_x$ reduction, antibacterial properties and reactivity in fission gas capture

Understanding how the size and structure of NPs evolve during synthesis and
how they are influenced by a support is critically important for optimization of their activity.

Control nanoparticle synthesis, crystalline porous supports, such as zeolites,
with well-defined cavities, provide a unique means of confining particle growth

Zeolite-supported metal clusters find application in selective catalysis, gas separation,
and photocatalysis

***Herein, we present an ongoing in situ study of the parameters that determine the mechanisms of NP growth and migration inside zeolite pores***

# *Broader Question*: Does Dehydration play a role in Ag-Zeolite nanoparticle formation?

**X-ray see heavy species well (Ag) but not the surface molecules ($H_2O$, OH, etc) that control the surface chemistries of the zeolites:**

**PDF + DRIFTS provides both complimentary methods**

**Ag nanoparticle formation induced by:** Reduction or Dehydration?

**Experiment:**

Variable temperature PDF + DRIFTS studies in reducing & inert atmosphere

- Three zeolites of differing framework and pores structure, and Si/Al ratio
- Heat 25 - 330°C while collecting data
- Monitor NP formation with transitions in water/hydroxides bonding & presence in zeolite
- Determine most important parameters & mechanisms

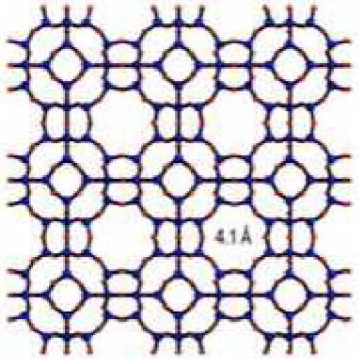


LTA (A)
Si/Al = 1

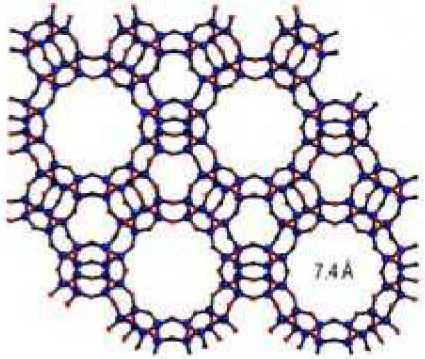


FAU (Y)
Si/Al = 2.4

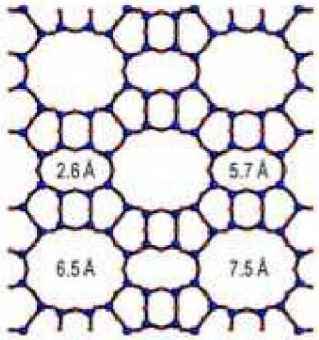


MOR
Si/Al = 5

**Use of Zeolites:** different chemistries (Si/Al ratios) and pore structures

**Use of Ag NPs:** ease of nanoparticle growth in zeolites and also for practical applications

# Filling in the missing pieces – PDF + IR

*Complementary insights from simultaneous IR spectroscopy*

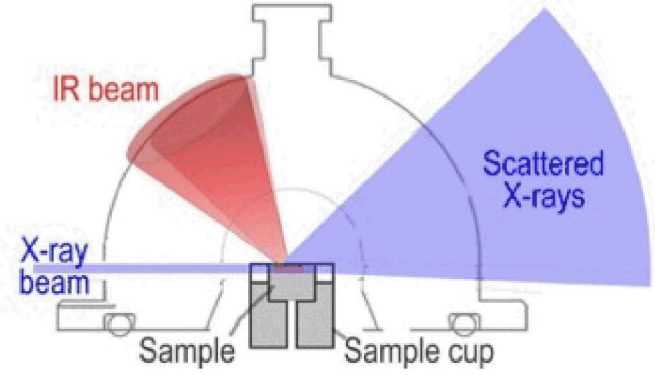


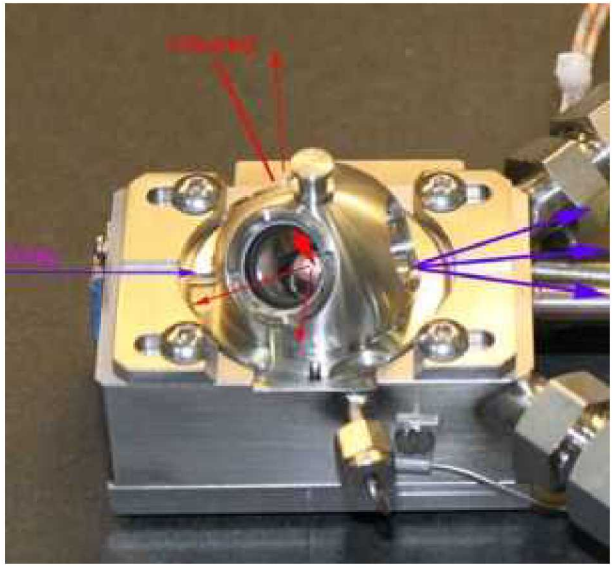

*DRIAD-X: Diffuse Reflectance Infrared Angular Dispersive X-ray Studies*

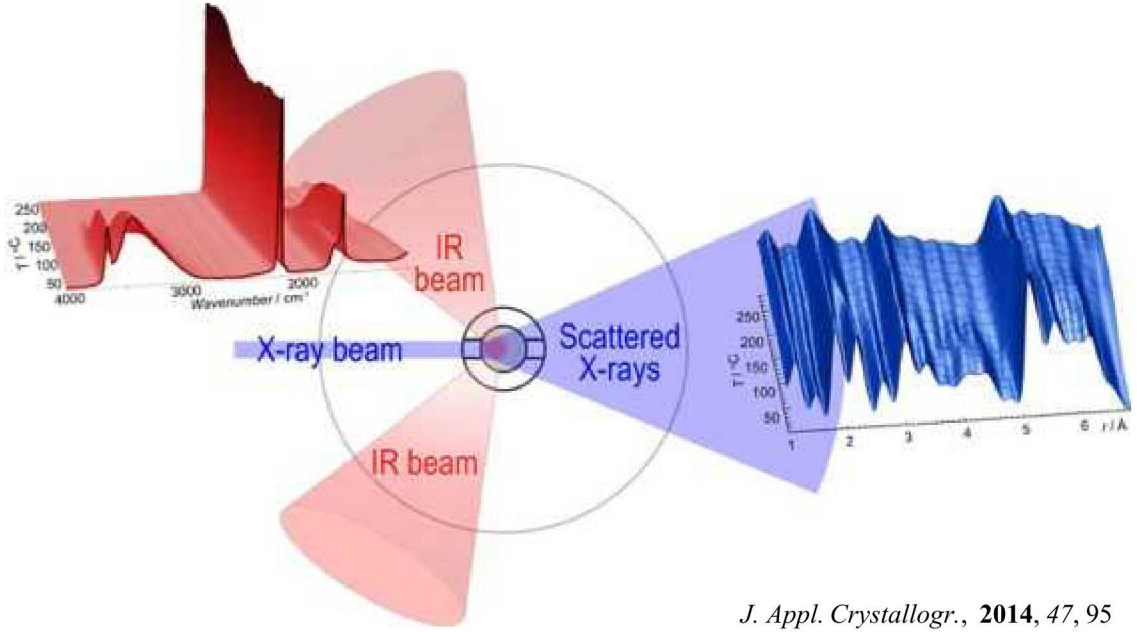


*J. Appl. Crystallogr.*, **2014**, *47*, 95

- PDF dominated by high Z species, no info on molecular chemistry
- Infra-red spectroscopy is sensitive to $H_2O$/OH molecular speciation
- PDF (transmission) & IR (diffuse reflectance) measurements are geometrically compatible.
- PDF + IR measurements can be performed **simultaneously** on the same sample region without compromise to the data

# Nanoparticle Growth in Aluminosilicate Zeolites

## (1) Chemistry of Framework

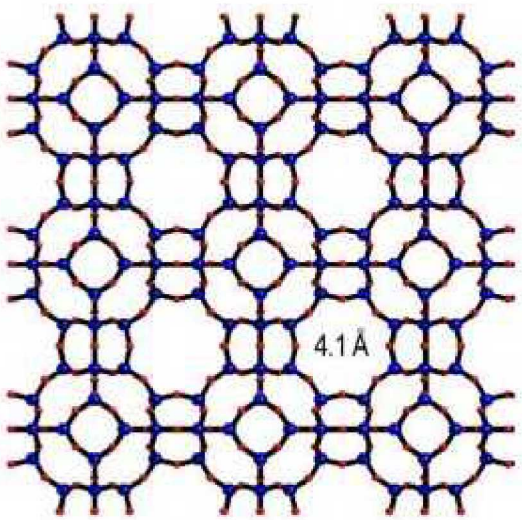


LTA (A)
Si/Al = 1

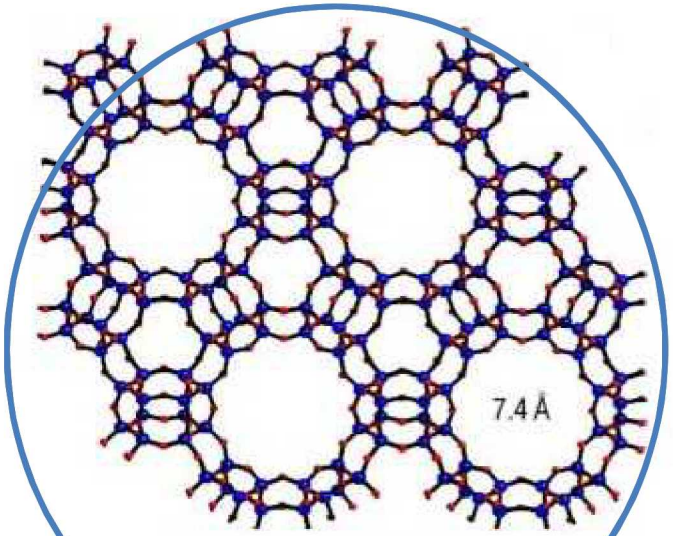


FAU (Y)
Si/Al = 2.4

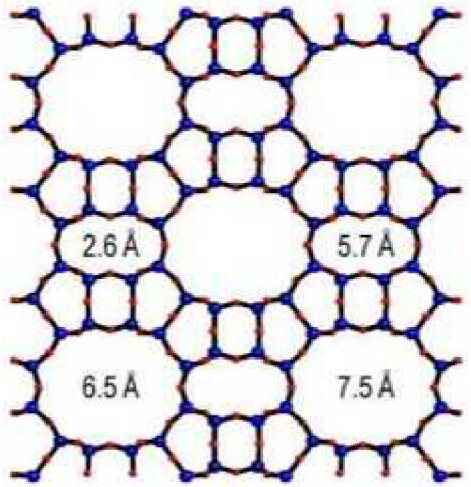


MOR
Si/Al = 5

## (2) Chemistry of the reduction:

Autoreduction = Temperature with He

Reduction – $H_2$ reducing gas with temperature

*Focus Today.*
Data compiled for all 3 zeolites and 2 chemistries

# In-depth PDF + IR analysis of FAU Y

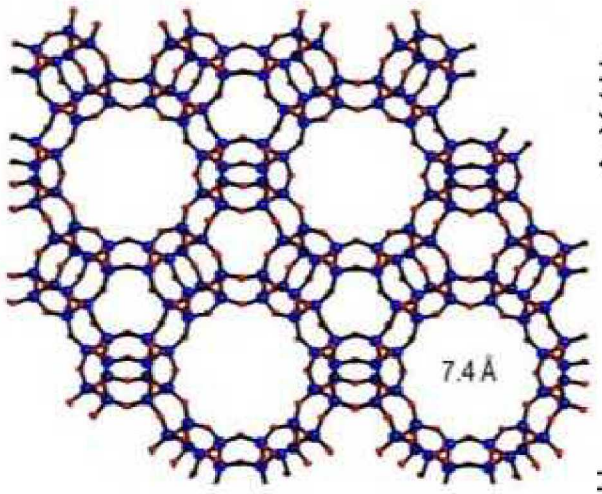


FAU (Y)

Si/Al = 2.4

Small clusters dominate over large temp range

PDF

DRIFTS

AgY / He

AgY / $H_2$

Small clusters & larger nanoparticles exist ~ in parallel

What does the IR tell us is happening simultaneously with the PDF?

# FAU Y: Key Observations from the IR

Autoreduction (He)

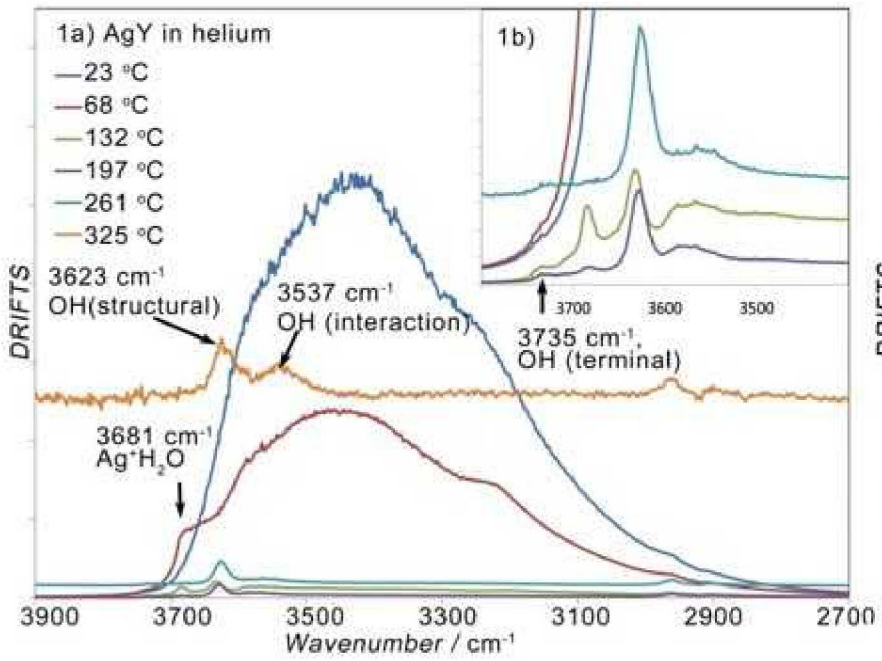


Reduction ($H_2$)

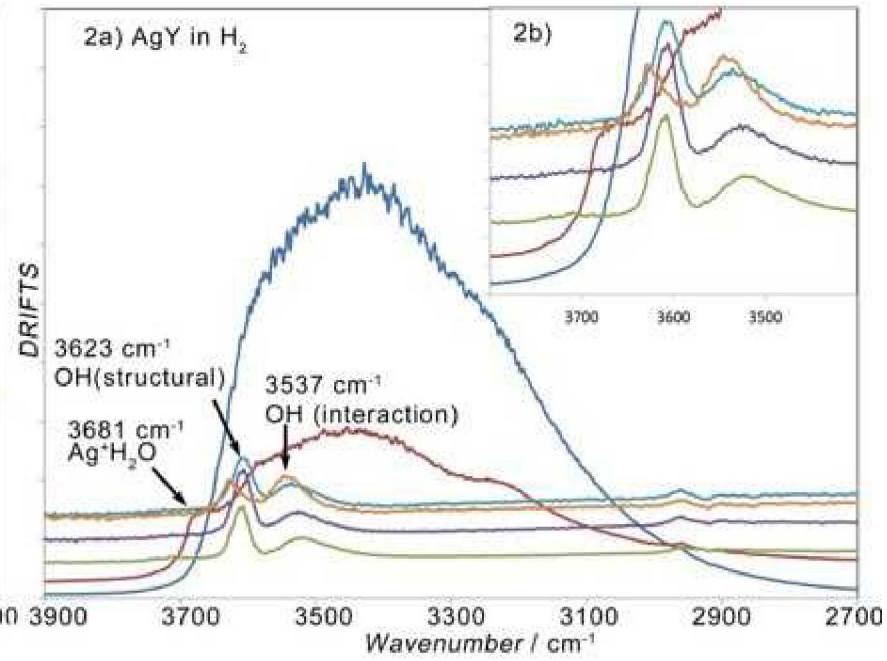


Assignments

- 3623 $cm^{-1}$ = structural hydroxyls
- 3537 $cm^{-1}$ = interaction of structural hydroxyls (from reduction of the $Ag^+$)
- 3681 $cm^{-1}$ = $Ag^+$-$H_2O$
- 3735 $cm^{-1}$ = terminal hydroxyls
- Baseline increases at end (reflects reduced reflectivity following NP formation)

# Detailed analysis for AgY in He (AutoReduction, Temperature Dependence)

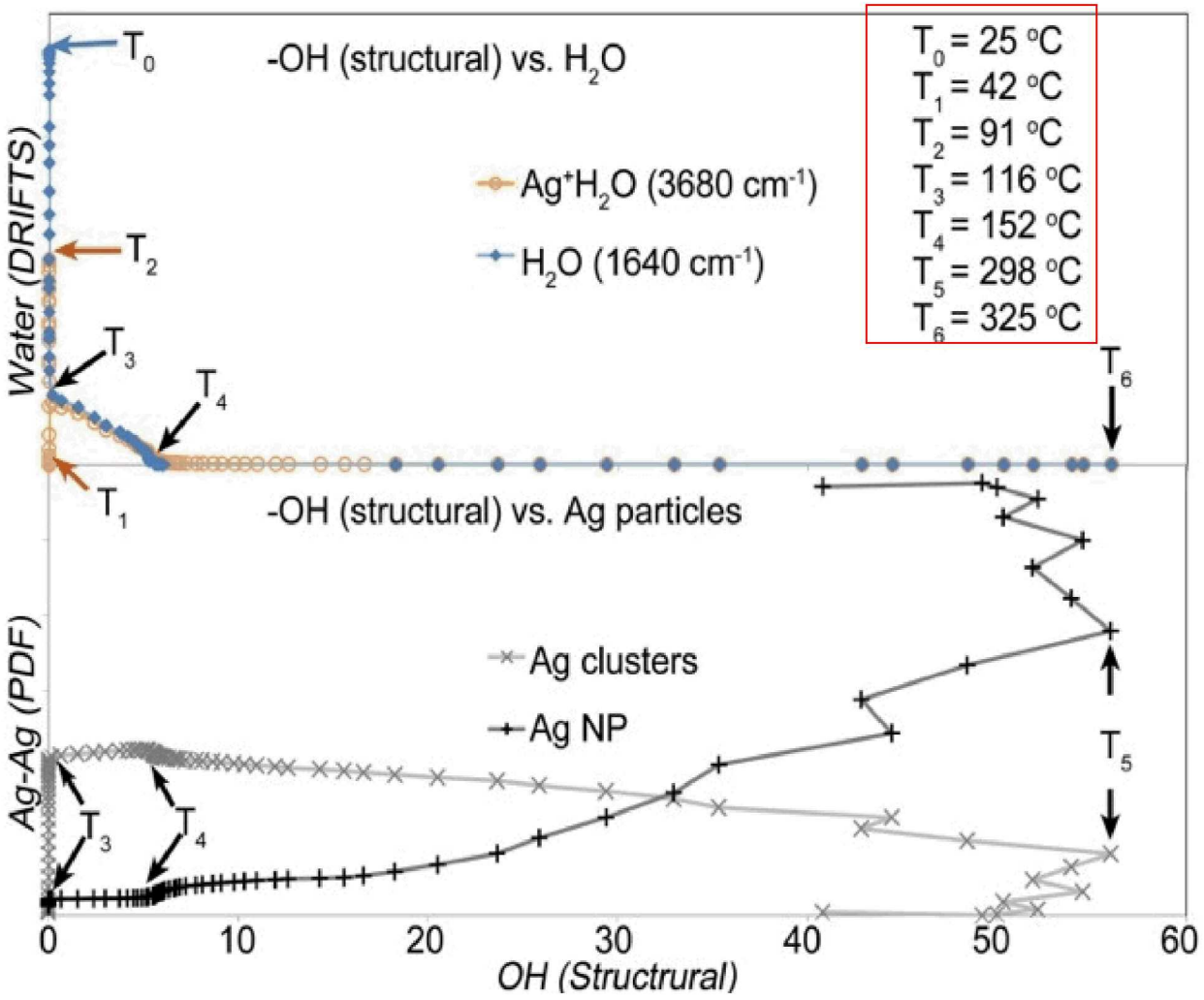

# Detailed analysis for AgY in He (AutoReduction, Temperature Dependence)

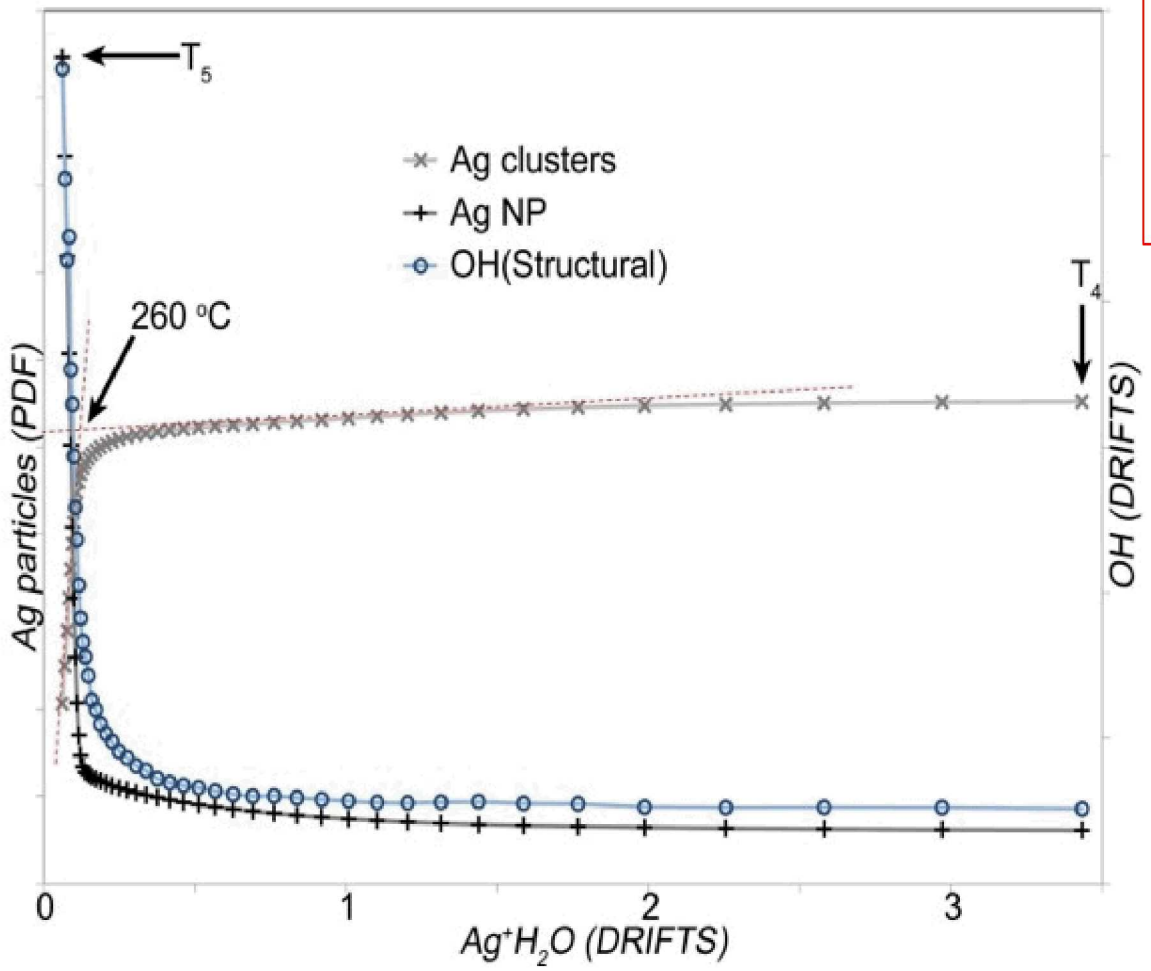


$T_0$ = 25 °C
$T_1$ = 42 °C
$T_2$ = 91 °C
$T_3$ = 116 °C
$T_4$ = 152 °C
$T_5$ = 298 °C
$T_6$ = 325 °C

# AgY Autoreduction (Temperature Dependence)

$T_0$ = 25 °C
$T_1$ = 42 °C
$T_2$ = 91 °C
$T_3$ = 116 °C
$T_4$ = 152 °C
$T_5$ = 298 °C
$T_6$ = 325 °C

• **$T_1$-$T_2$:** no framework hydroxyl formed; Ag clusters & $Ag^+H_2O$ start to grow, reach max 91°C. Ag clusters are Ag cationic clusters associated with $H_2O$.
In this temperature range, water peak at 1640 $cm^{-1}$ drop dramatically.
No Ag nanoparticles formed.

• **$T_2$-$T_3$:** $Ag^+H_2O$ drops rapidly; Ag ion clusters growing to maxima. Still no framework -OH.
Water molecules desorbed from the silver cationic clusters.

• **$T_3$-$T_4$:** framework -OH started to form while Ag clusters population kept constant, no Ag NP formed.
The small amount of hydroxyls formed implies a partial reduction of the Ag ion clusters:

$$2(Ag^+\text{-}Z\text{-}O^-) + H_2O \rightarrow \tfrac{1}{2}\, O_2 + 2Ag + 2Z\text{-}OH$$

• **$T_4$-$T_5$:** Ag clusters diminish, Ag NP increased slowly. The much higher slope of –OH vs. $Ag^+H_2O$ formation indicates more Ag cations were reduced, rapid Ag cluster decrease and Ag NPs increase.
Ag cation reduction is the limiting step for Ag clusters concentration decreasing
Ag NPs form because the Ag cationic clusters are stabilized by water.

• **$T_5$-$T_6$:** Framework –OH started to decay suggests dehydroxylation reaction occurs. Ag NPs grow.
Ag clusters continue to decrease, suggesting a new autoreduction mechanism is dominant at this temperature range:

$$2(Ag^+\text{-}Z\text{-}O^-) \rightarrow \tfrac{1}{2}\, O_2 + 2Ag + Z\text{-}O^- + Z^+$$

# Proposed Mechanism of AgY Autoreduction

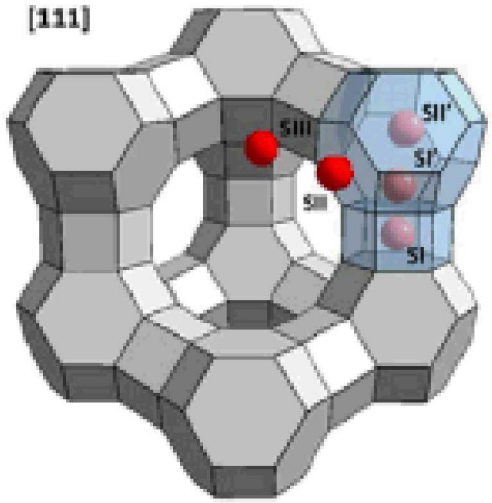


Temperature Dependence

$$n\,\mathrm{Ag}^{+} + m\mathrm{H_2O} \xrightarrow{T_1 \sim T_2}$$

$$\mathrm{Ag}_n^{n+}.mH_2O \xrightarrow{T_2 \sim T_3}$$

$$\mathrm{Ag}_n^{n+}.p\mathrm{H_2O} \xrightarrow{T_3 \sim T_4}$$

$$\mathrm{Ag}_n^{q+}.r\mathrm{H_2O} + a\mathrm{Z-OH} \xrightarrow{T_4 \sim 260^{\circ}\mathrm{C}}$$

$$\mathrm{Ag}_f^{t+}.s\mathrm{H_2O} + d\mathrm{Ag}^0(\mathrm{Ag\ NPs}) + b\mathrm{Z-OH} \xrightarrow{260^{\circ}\mathrm{C} \sim T_5}$$

$$h\mathrm{Ag}^0(\mathrm{AgNPs}) + cZ - \mathrm{OH} + \mathrm{Ag}^{+} \xrightarrow{T_5 \sim T_6}$$

$$k\mathrm{Ag}^0(\mathrm{AgNPs}) + \mathrm{Z-O}^{-} + \mathrm{Z}^{+}$$

# Correlate changes in Ag and $H_2O$/OH populations

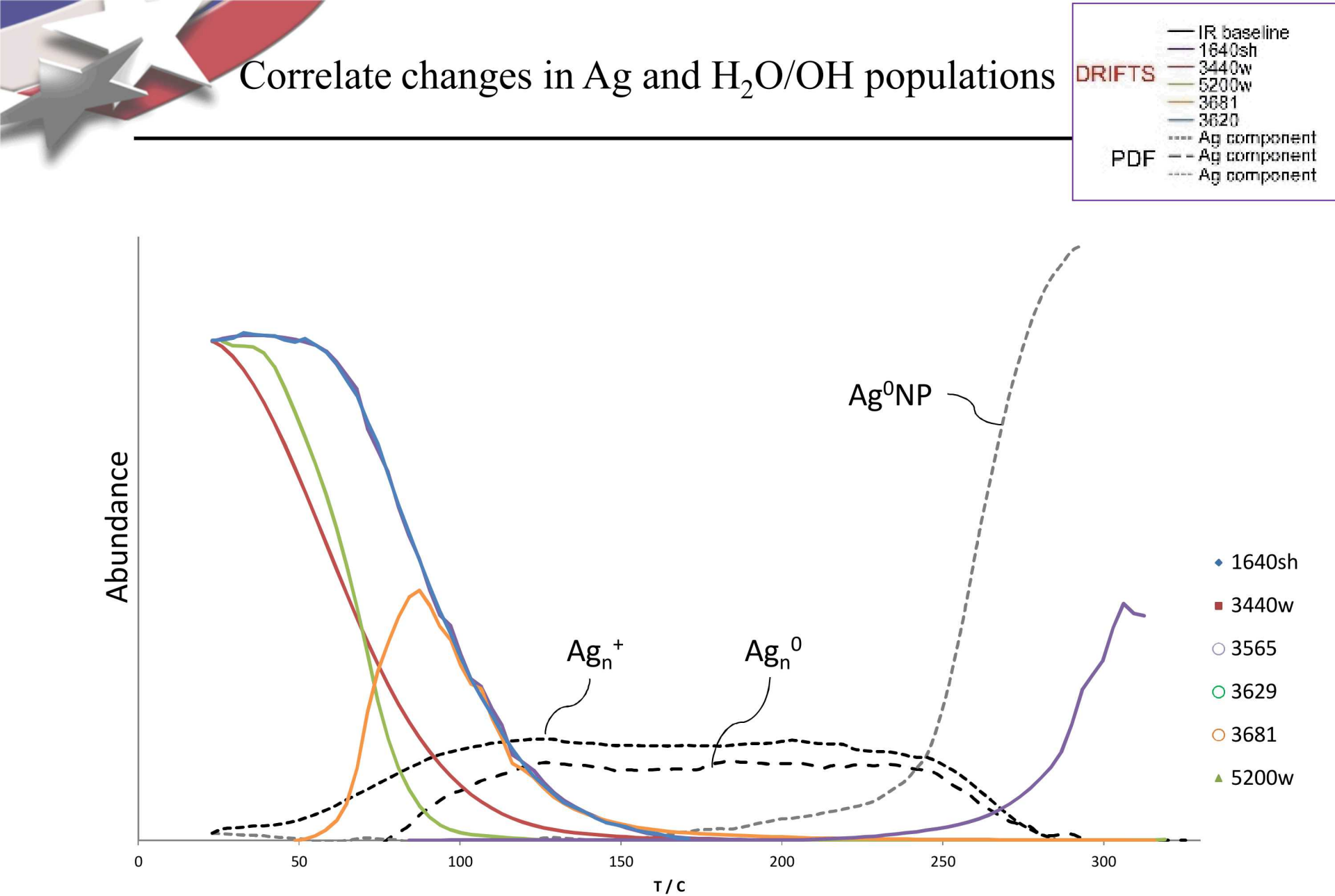




T. M. Nenoff, tmnenof@sandia.gov

44

# Nanoparticle Growth in Aluminosilicate Zeolites

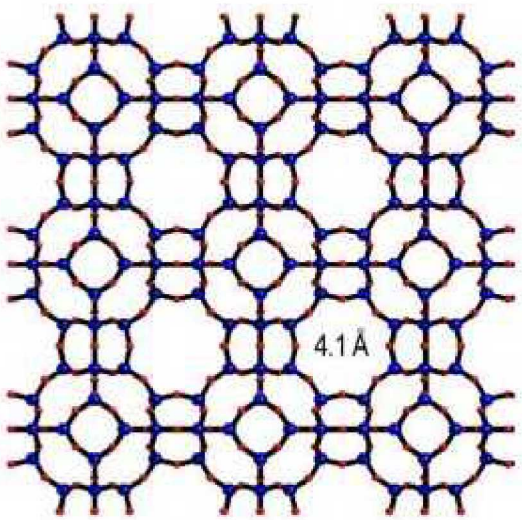


LTA (A)
Si/Al = 1

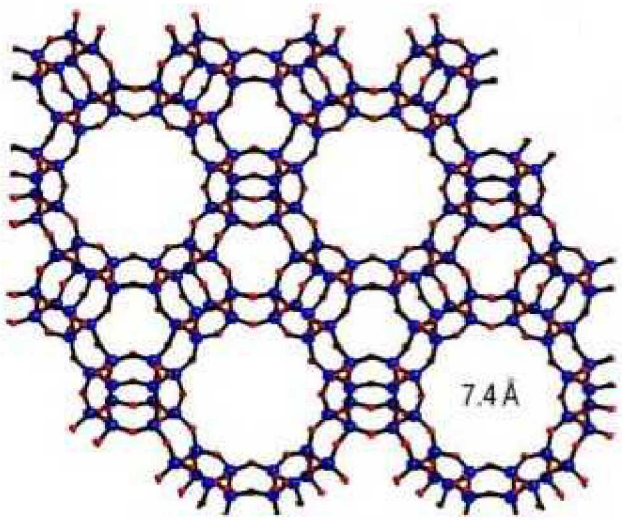


FAU (Y)
Si/Al = 2.4

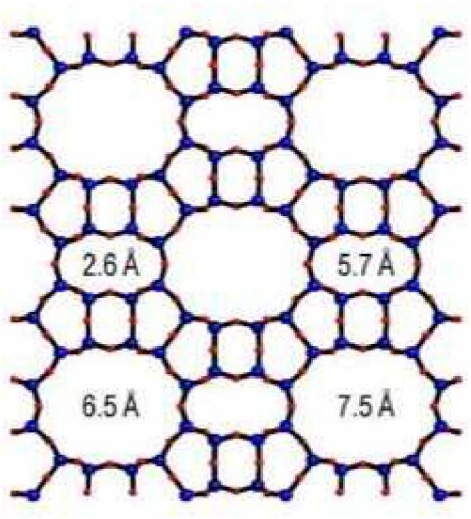


MOR
Si/Al = 5

**Data sets are very complex and somewhat overwhelming**
**Deciphering data sets to simplify the interpretation**

# Quantifying Changes:
# to be used in correlation Analysis

DRIFTS: IR baseline, 1640sh, 3440w, 5200w, 3681, 3620
PDF: Ag component, Ag component, Ag component

For autoreduction, the onset of large NP formation is ~275°C.
Small clusters dominate and are stable over a wide temperature range (~125-225°C)

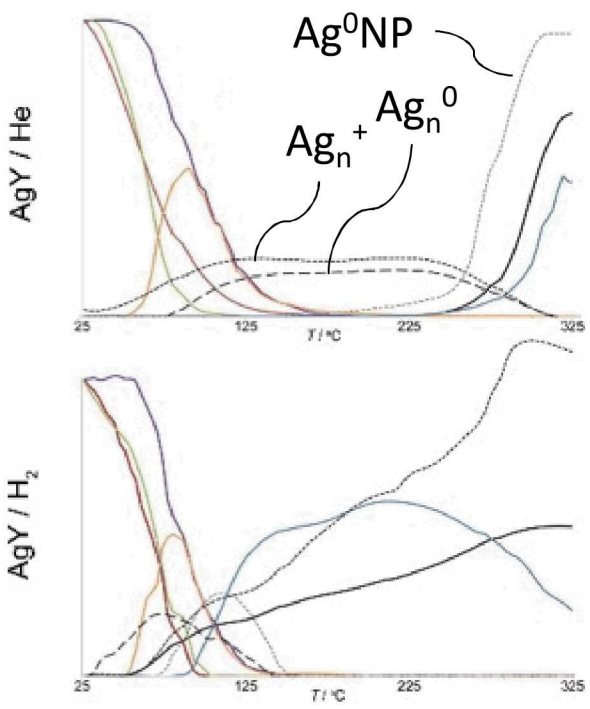


Si/Al = 2.4

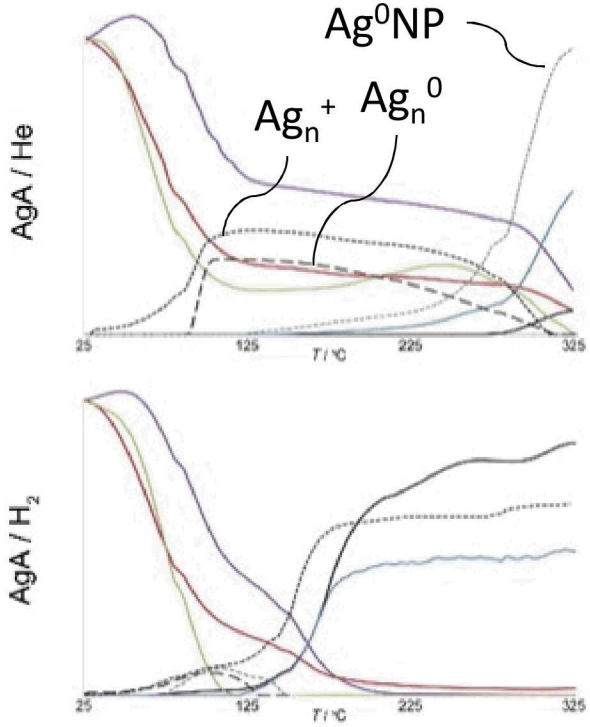


Si/Al = 1

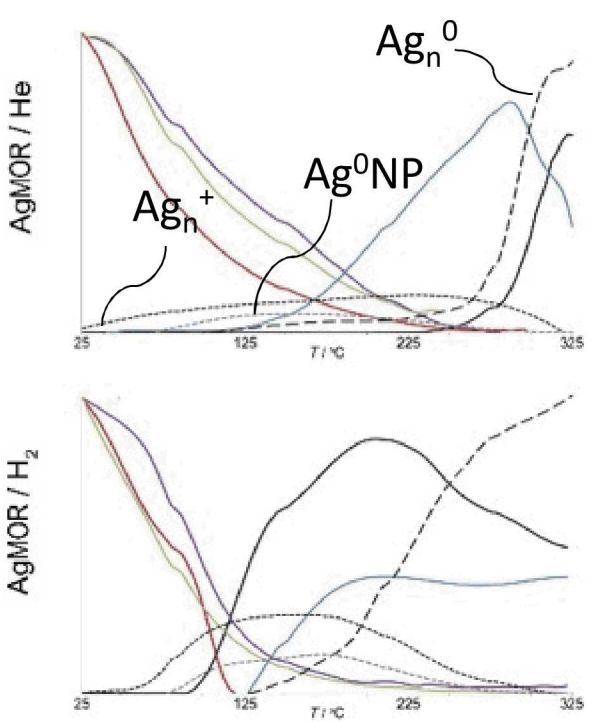


Si/Al = 5

Under reducing conditions, clusters and large NP form approximately in parallel.
Ag clusters persist to higher temperatures for higher Al ratio zeolites

# Correlating Parameters: Which Parameters change together? Insights from simultaneous data collection

Short Cut way to see most important factors

Pink = -ve correlation
Blue = +ve correlation
What changes occur in parallel? Anti-parallel?

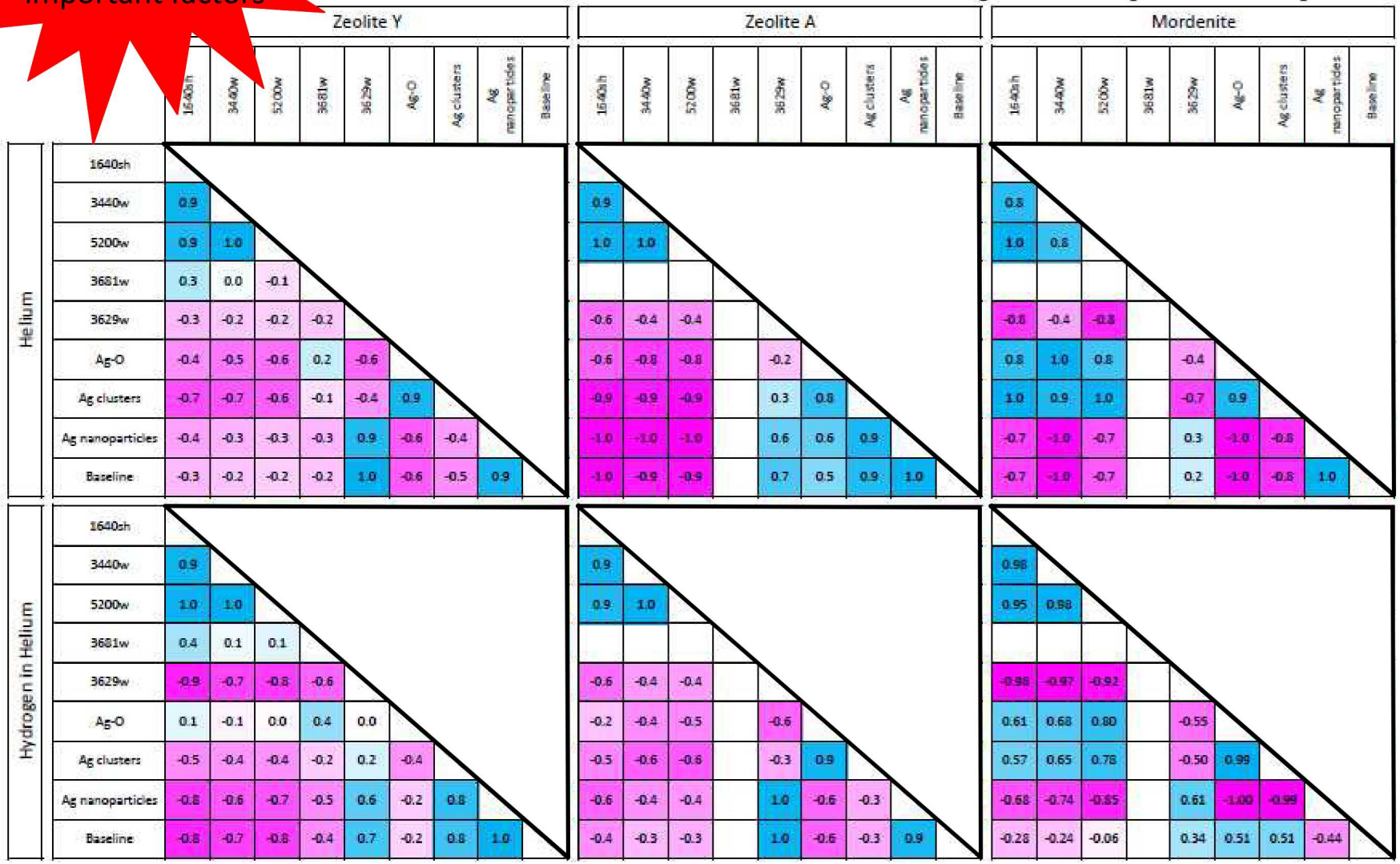

| | | Zeolite Y | | | | | | | | | Zeolite A | | | | | | | | | Mordenite | | | | | | | | |
|---|---|---|---|---|---|---|---|---|---|---|---|---|---|---|---|---|---|---|---|---|---|---|---|---|---|---|---|---|
| | | 1640sh | 3440w | 5200w | 3681w | 3629w | Ag-O | Ag clusters | Ag nanoparticles | Baseline | 1640sh | 3440w | 5200w | 3681w | 3629w | Ag-O | Ag clusters | Ag nanoparticles | Baseline | 1640sh | 3440w | 5200w | 3681w | 3629w | Ag-O | Ag clusters | Ag nanoparticles | Baseline |
| Helium | 1640sh | | | | | | | | | | | | | | | | | | | | | | | | | | | |
| | 3440w | 0.9 | | | | | | | | | 0.9 | | | | | | | | | 0.8 | | | | | | | | |
| | 5200w | 0.9 | 1.0 | | | | | | | | 1.0 | 1.0 | | | | | | | | 1.0 | 0.8 | | | | | | | |
| | 3681w | 0.3 | 0.0 | -0.1 | | | | | | | | | | | | | | | | | | | | | | | | |
| | 3629w | -0.3 | -0.2 | -0.2 | -0.2 | | | | | | -0.6 | -0.4 | -0.4 | | | | | | | -0.8 | -0.4 | -0.8 | | | | | | |
| | Ag-O | -0.4 | -0.5 | -0.6 | 0.2 | -0.6 | | | | | -0.6 | -0.8 | -0.8 | | -0.2 | | | | | 0.8 | 1.0 | 0.8 | | -0.4 | | | | |
| | Ag clusters | -0.7 | -0.7 | -0.6 | -0.1 | -0.4 | 0.9 | | | | -0.9 | -0.9 | -0.9 | | 0.3 | 0.8 | | | | 1.0 | 0.9 | 1.0 | | -0.7 | 0.9 | | | |
| | Ag nanoparticles | -0.4 | -0.3 | -0.3 | -0.3 | 0.9 | -0.6 | -0.4 | | | -1.0 | -1.0 | -1.0 | | 0.6 | 0.6 | 0.9 | | | -0.7 | -1.0 | -0.7 | | 0.3 | -1.0 | -0.8 | | |
| | Baseline | -0.3 | -0.2 | -0.2 | -0.2 | 1.0 | -0.6 | -0.5 | 0.9 | | -1.0 | -0.9 | -0.9 | | 0.7 | 0.5 | 0.9 | 1.0 | | -0.7 | -1.0 | -0.7 | | 0.2 | -1.0 | -0.8 | 1.0 | |
| Hydrogen in Helium | 1640sh | | | | | | | | | | | | | | | | | | | | | | | | | | | |
| | 3440w | 0.9 | | | | | | | | | 0.9 | | | | | | | | | 0.98 | | | | | | | | |
| | 5200w | 1.0 | 1.0 | | | | | | | | 0.9 | 1.0 | | | | | | | | 0.95 | 0.98 | | | | | | | |
| | 3681w | 0.4 | 0.1 | 0.1 | | | | | | | | | | | | | | | | | | | | | | | | |
| | 3629w | -0.9 | -0.7 | -0.8 | -0.6 | | | | | | -0.6 | -0.4 | -0.4 | | | | | | | -0.98 | -0.97 | -0.92 | | | | | | |
| | Ag-O | 0.1 | -0.1 | 0.0 | 0.4 | 0.0 | | | | | -0.2 | -0.4 | -0.5 | | -0.6 | | | | | 0.61 | 0.68 | 0.80 | | -0.55 | | | | |
| | Ag clusters | -0.5 | -0.4 | -0.4 | -0.2 | 0.2 | -0.4 | | | | -0.5 | -0.6 | -0.6 | | -0.3 | 0.9 | | | | 0.57 | 0.65 | 0.78 | | -0.50 | 0.99 | | | |
| | Ag nanoparticles | -0.8 | -0.6 | -0.7 | -0.5 | 0.6 | -0.2 | 0.8 | | | -0.6 | -0.4 | -0.4 | | 1.0 | -0.6 | -0.3 | | | -0.68 | -0.74 | -0.85 | | 0.61 | -1.00 | -0.99 | | |
| | Baseline | -0.8 | -0.7 | -0.8 | -0.4 | 0.7 | -0.2 | 0.8 | 1.0 | | -0.4 | -0.3 | -0.3 | | 1.0 | -0.6 | -0.3 | 0.9 | | -0.28 | -0.24 | -0.06 | | 0.34 | 0.51 | 0.51 | -0.44 | |

# Correlating Parameters: Which Parameters change together? Insights from simultaneous data collection

Removal of water correlates with 100% NP formation

Pink = -ve correlation
Blue = +ve correlation
What changes occur in parallel? Anti-parallel?

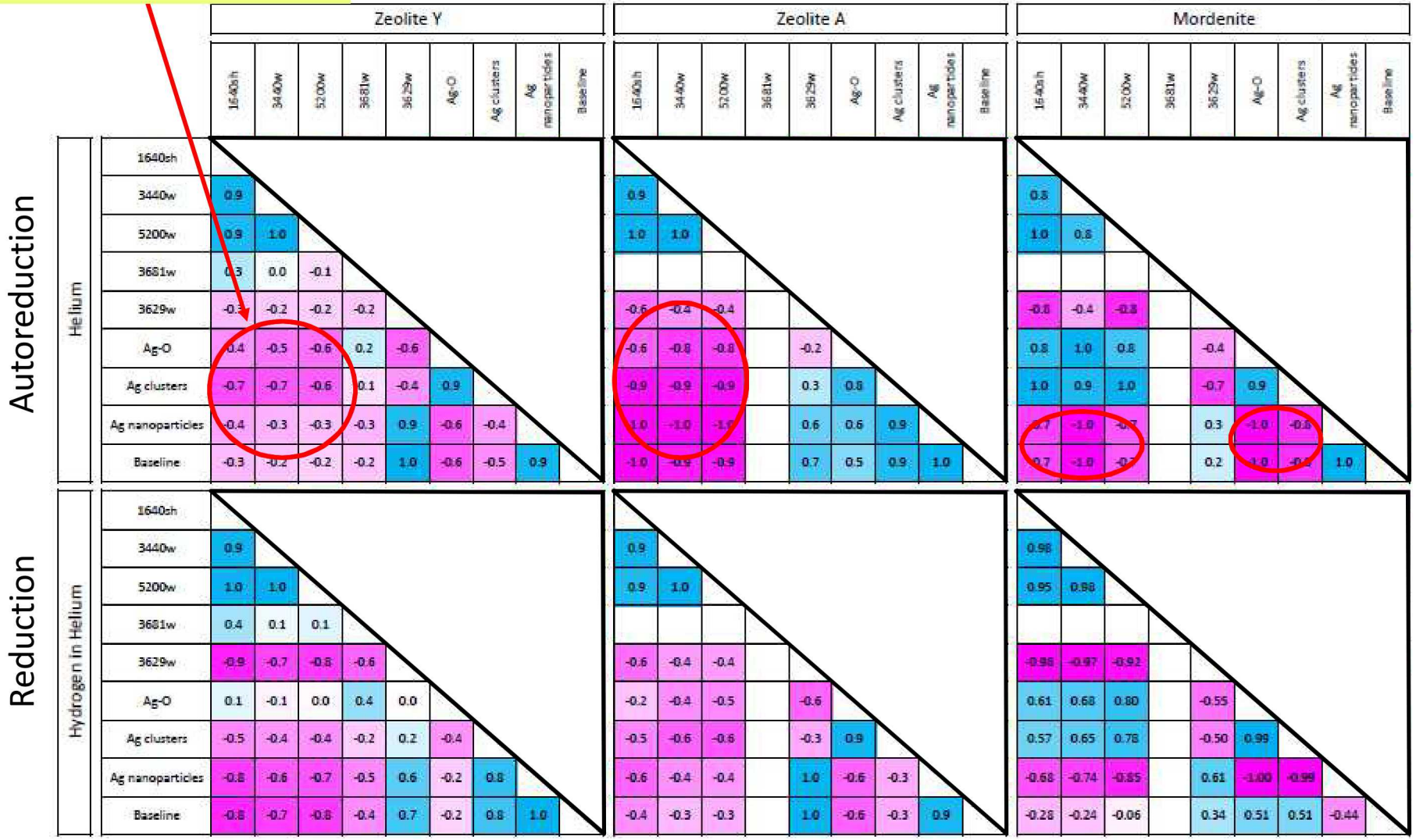

# Comparing AutoReduction and $H_2$

+/- = large difference in mechanism between He and $H_2$


Example of insights: In Y,

under He, the Ag clusters have $H_2O$ bound, Ag clusters are consumed to form Ag NP (sequential)

under $H_2$, the Ag clusters and Ag NP form at more similar times. Ag clusters not bounded by $H_2O$

# Conclusion

*Fission Gas selectivity for Capture and Storage is highly dependent upon local nanoscale interactions*

Use of **impedance spectroscopy** enables direct electrical readout of iodine gas presence,
in ambient conditions of temperature and humidity
this is due to the *highly polarizable nature of* $I_2$

Success with IS is ensured due to the ability to test 100 kHz – 1 Hz in 10 s using FFT methods

**Nanoparticle Growth:**

While PDF/X-rays enabled the determination of the nanoparticle growth, IR is needed to observe the softer molecules ($H_2O$, -OH) present during the NP formation and migration

Simultaneous PDF/DRIFTS are complimentary revealing NP formation and fate of occluded waters

**To Date:**

Pore size affects ease of hydroxides removal is hindered by "blocking" from formed Ag clusters/NPs

A: uniform pores – $H_2O$ trapped

MOR: intermediate pores – $H_2O$ less trapped

Y: varied pores – large escape pathways for $H_2O$

Appears Si/Al ratio has much more effect on reduction and growth of NPs than pore structure

eg., Ag clusters persist to higher temperatures with the higher ratio

Reducing conditions, NPs and clusters form together in all, but

Autoreduction (heating) contains a period of smaller clusters only, and only after water is driven off that NP mobility occurs

Autoreduction: 100°C Temp range only see small clusters without forming large NPs

# Acknowledgements


For Projects Highlighted herein

Sandia National Labs:
- Leo Small
- Dorina Sava Gallis
- Mark A. Rodriguez
- David X. Rademacher

APS/ANL:
- Karena W. Chapman
- Peter Chupas
- Kevin A. Beyer
- Saul H. Lapidus

Univ Idaho:
- Haiyan Zhao

Univ Warwick:
- M. A. Newton

Funding Agencies:
- SNL LDRD
- US DOE/NE - Fuel Cycle
- US State Dept - VFund


**Sandia National Labs**
**Albuquerque, New Mexico**

# Questions? / Thank you

# Example 1: AgI nanoparticle formation in MOR (from $Ag^+$-MOR + iodine species)

*JACS,* **2010**, *132*(26), 8897

*MMM,* **2014**, *200*, 297

## Ag-MOR + $I_2$

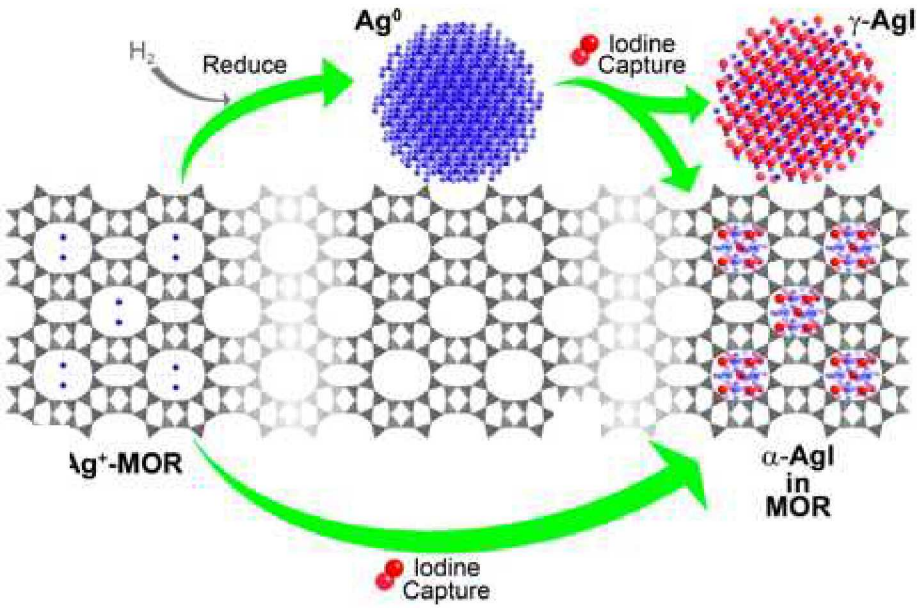


## Ag-MOR + $CH_3$-I

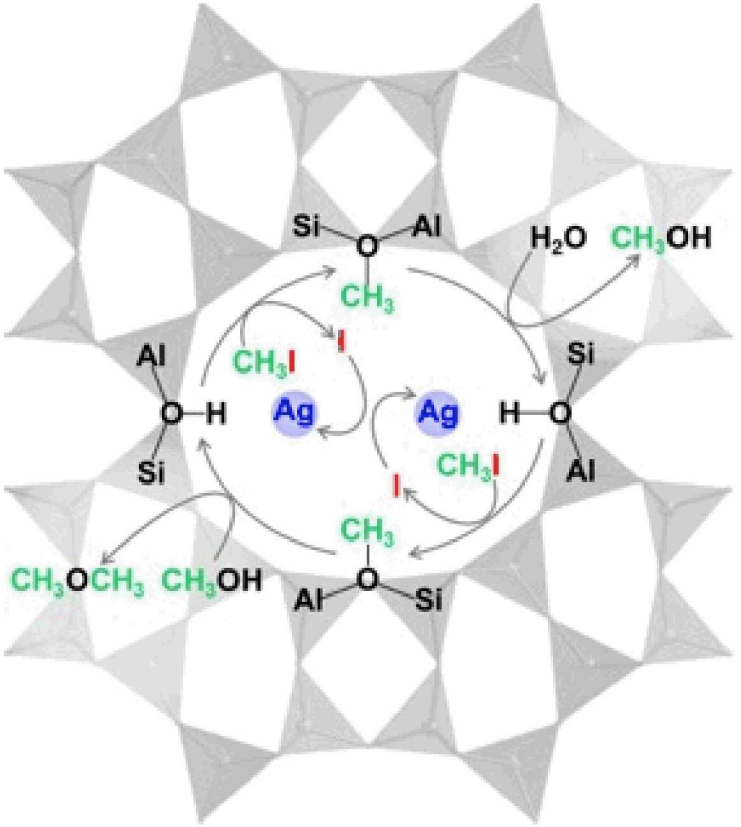


Mechanism of AgI formation & phase determination

# Example 2: Ag Nanoparticle Formation in Zeolite MOR (from $Ag^+$-MOR)

Study Conversion and Migration of $Ag^+$ to $Ag^\circ$ in MOR

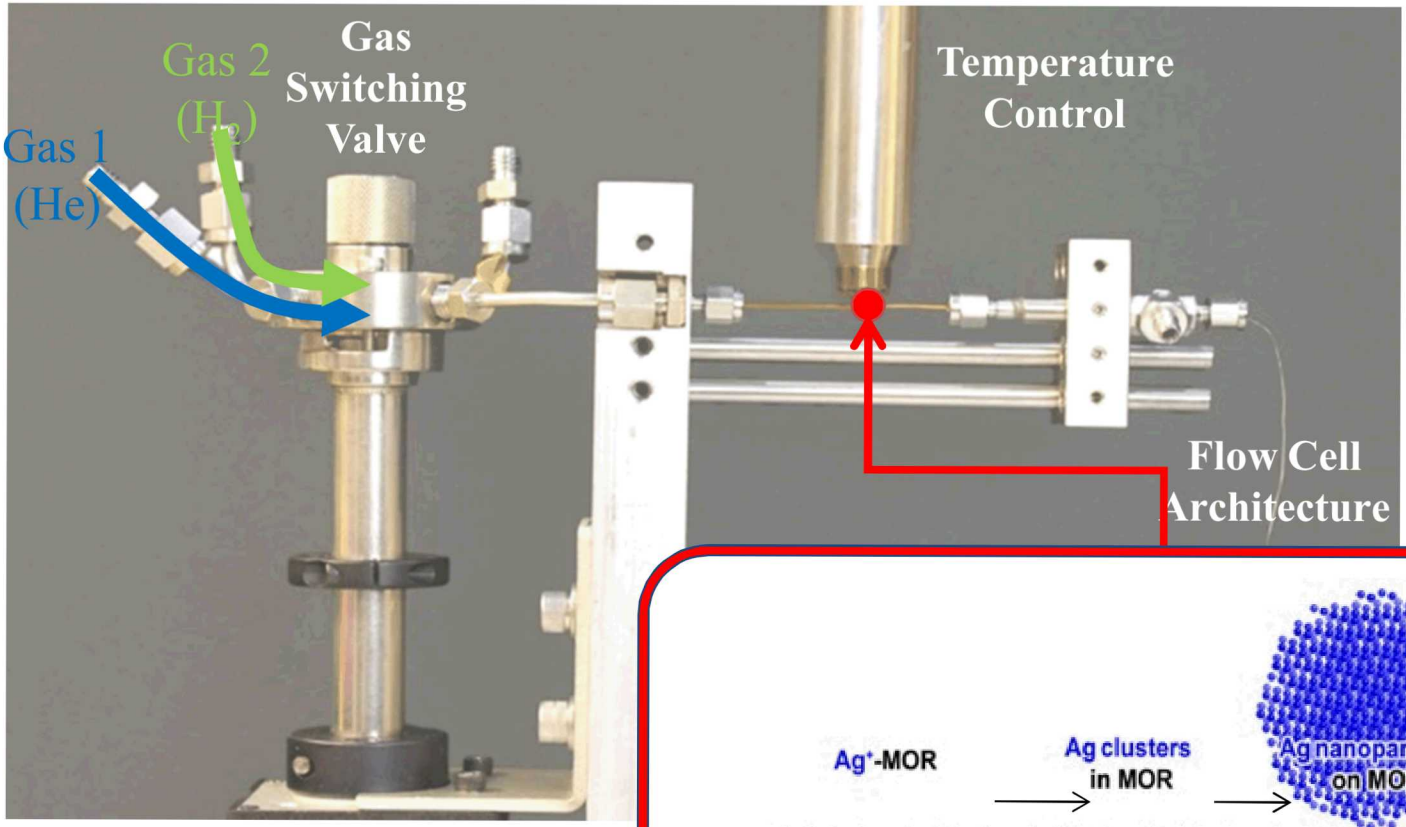


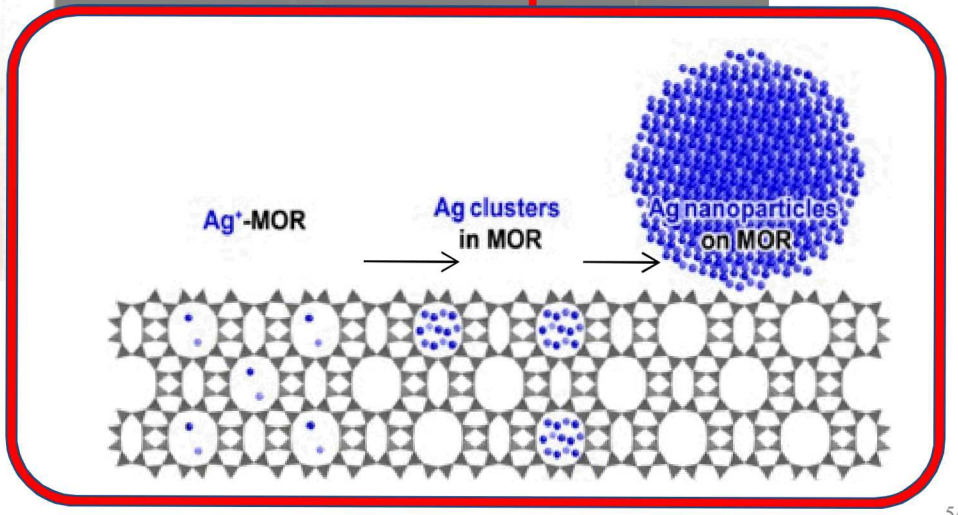


In situ $I_2$ sorption on Ag-MOR using PDF setup at 11-ID-B beamline at APS/ANL

# Multi-step Mechanism for Silver Particle Growth and Migration on a Porous Zeolite

i) $Ag^{+}$ reduction in 12MR and 8MR "Red star"
ii) Ag° migration from 8MR to 12MR
iii) Ag° form clusters within 12MR channels
iv) Clusters migrate to zeolite surface
v) Clusters aggregate as nanoparticles

Mechanism Pathway Determined

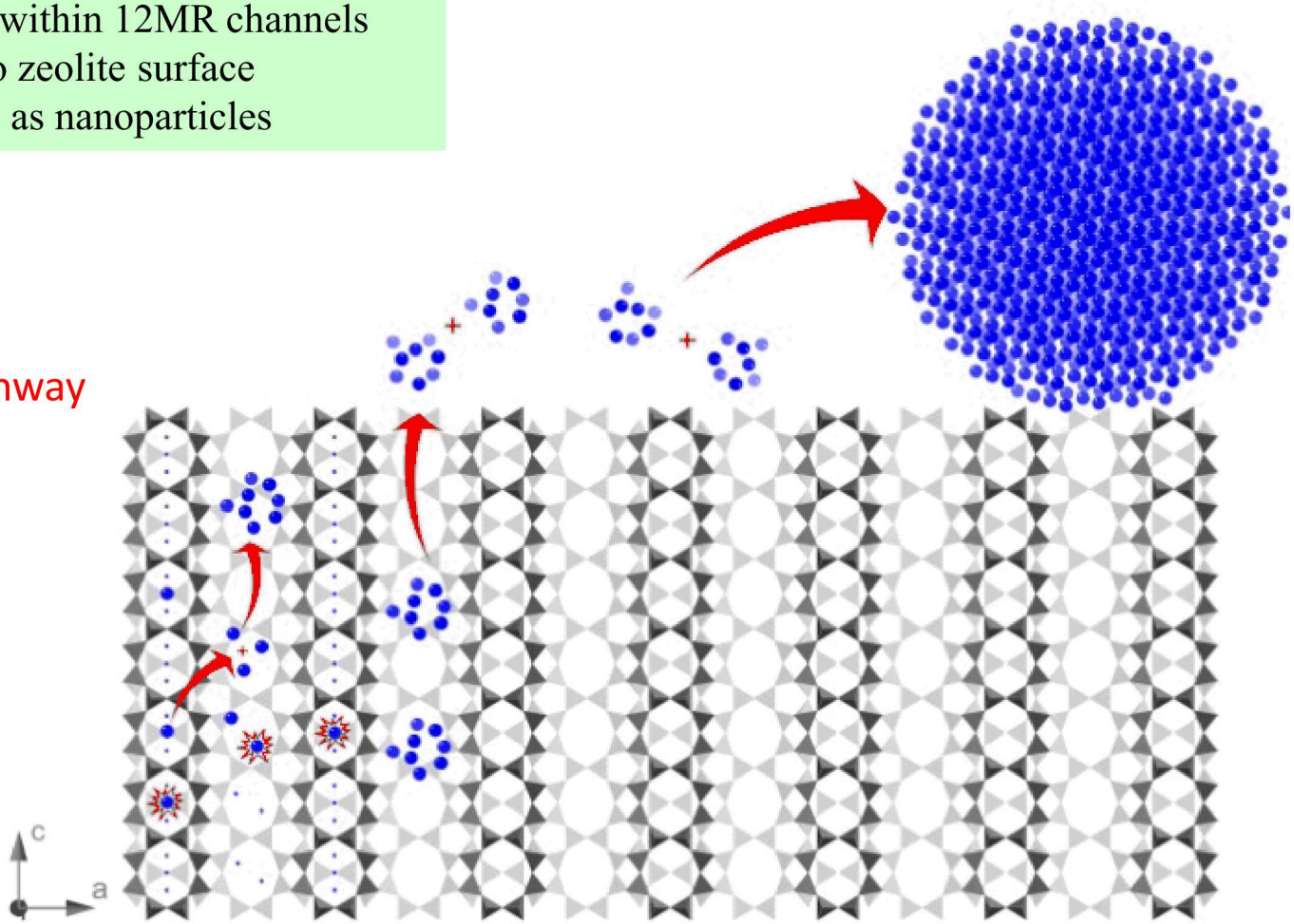




*J Phys Chem Letters*, **2011**, *2*, 2742

# Nanoparticle Growth in Aluminosilicate Zeolites

## (1) Chemistry of Framework

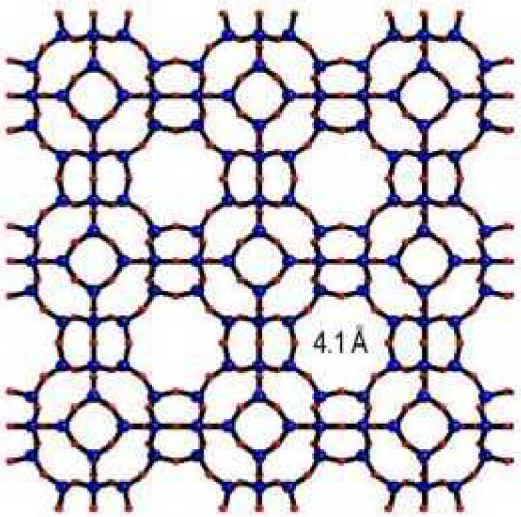


LTA (A)

Si/Al = 1

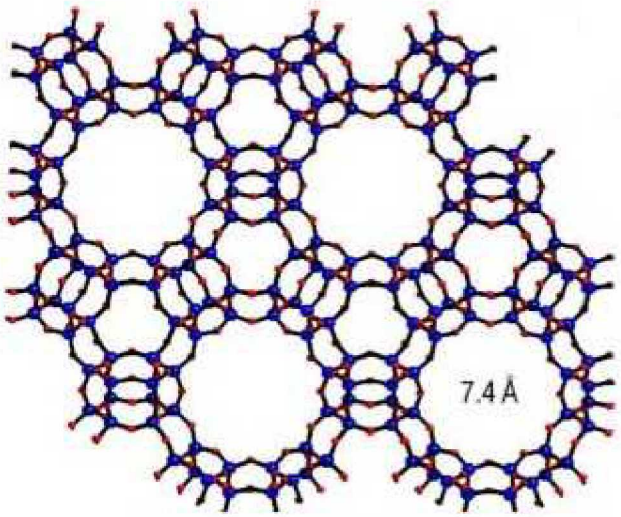


FAU (Y)

Si/Al = 2.4

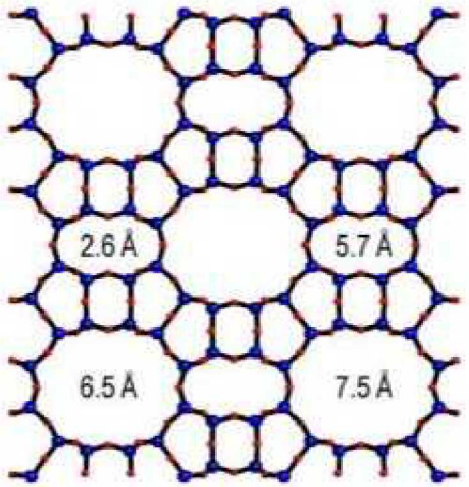


MOR

Si/Al = 5

## (2) Chemistry of the reduction:

Autoreduction = Temperature with He

Reduction – $H_2$ reducing gas with temperature

**How does framework chemistry and/or geometry play a role in NP formation?**

Comparison of
combined PDF & DRIFTS

Zeolites Y, A, MOR
in $H_2$ (reducing environment)
vs He (autoreduction/heat)

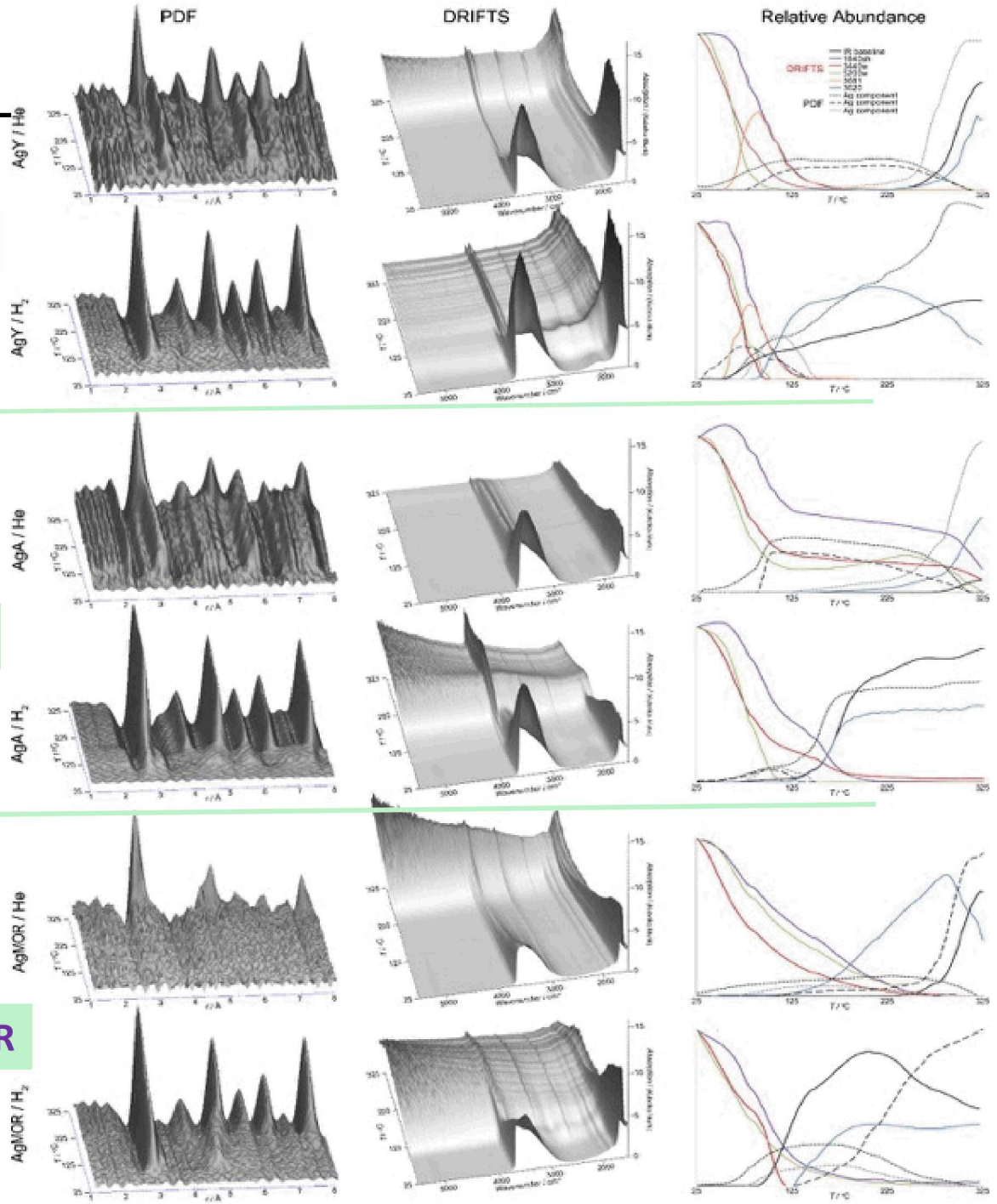


T. M. Nenoff, tmnenof@sandia.gov

# Quantifying Changes

DRIFTS: IR baseline, 1640sh, 3440w, 5200w, 3681, 3620
PDF: Ag component, Ag component, Ag component

For autoreduction, the onset of large NP formation is ~275°C.
Small clusters dominate and are stable over a wide temperature range (~125-225°C)

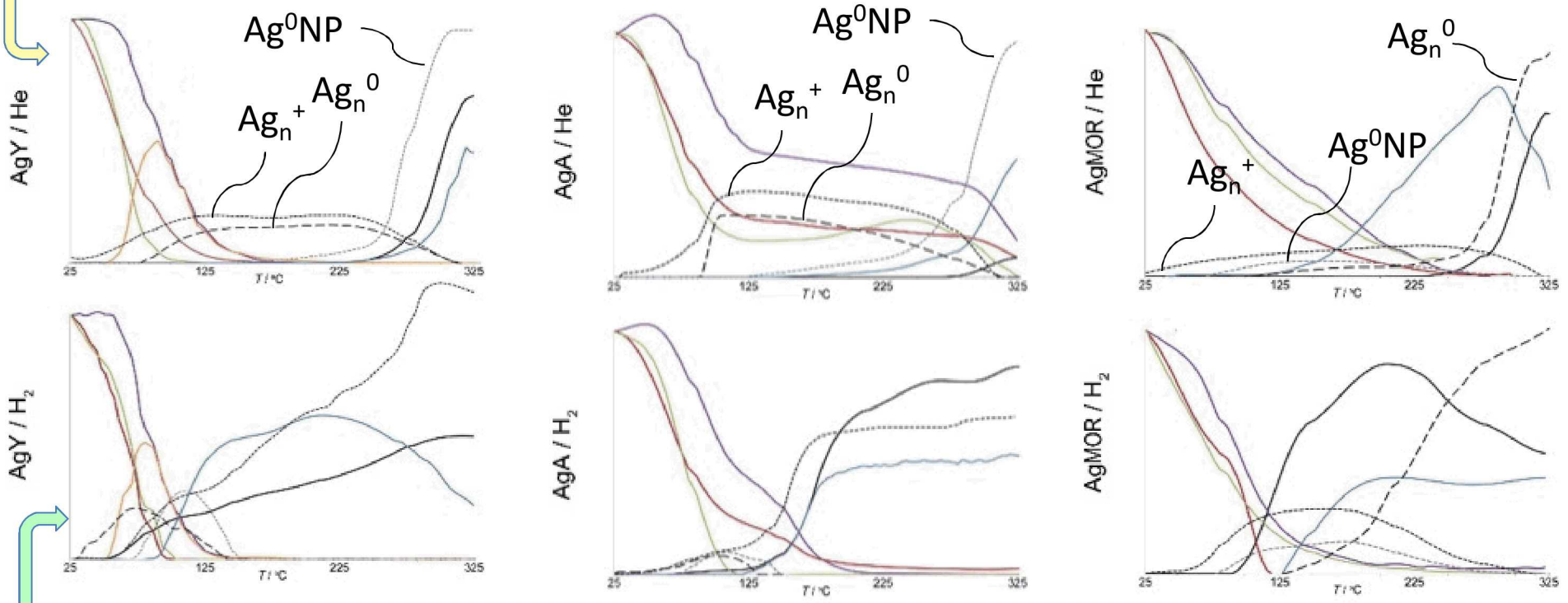


Under reducing conditions, clusters and large NP form approximately in parallel.
Ag clusters persist to higher temperatures for higher Al ratio zeolites

# Amorphous Carbon/Activated Charcoal: Active Capture of Iodine, and *Everything* else

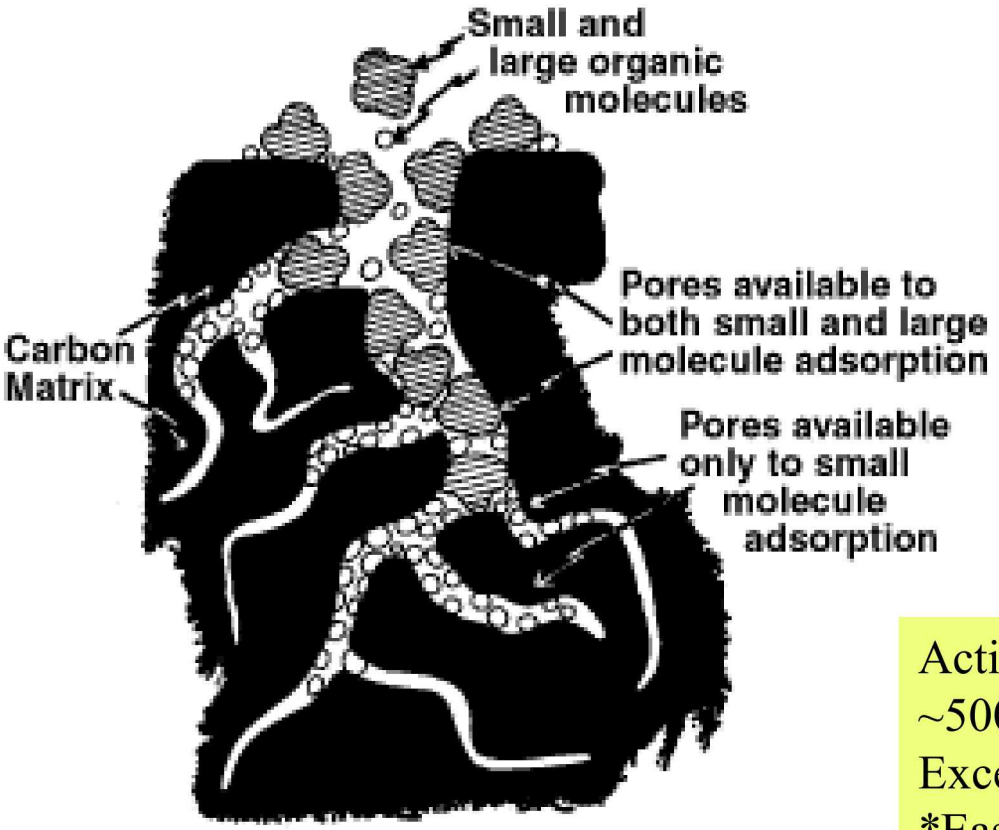


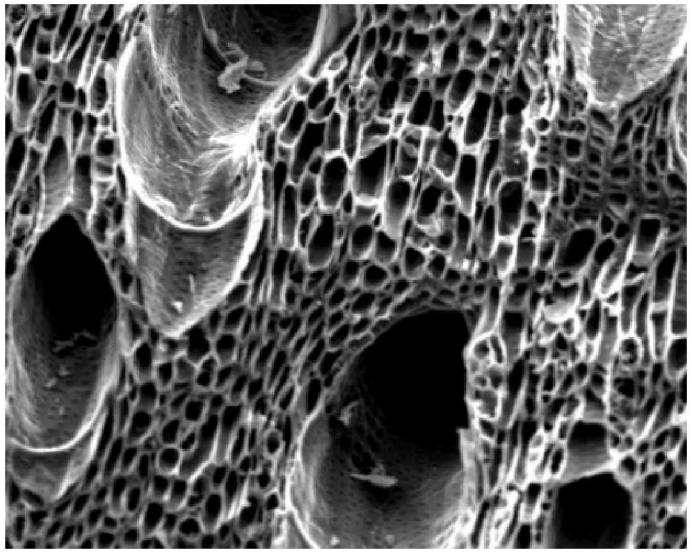

Activated Charcoals have mesoscale porosity,
~500 $m^2/g$ surface area
Exceptional adsorption, but no selectivity
*Easily "clogged"*

Most Charcoals are organic based,
Contain substantial quantities of natural iodine

# Structure-Property Relationships

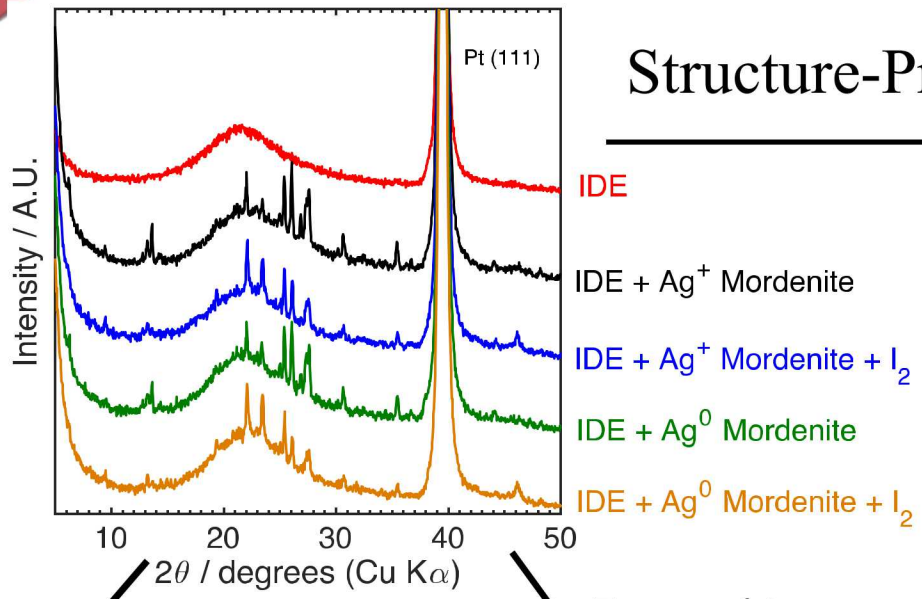


Zoomed in

Zoomed in

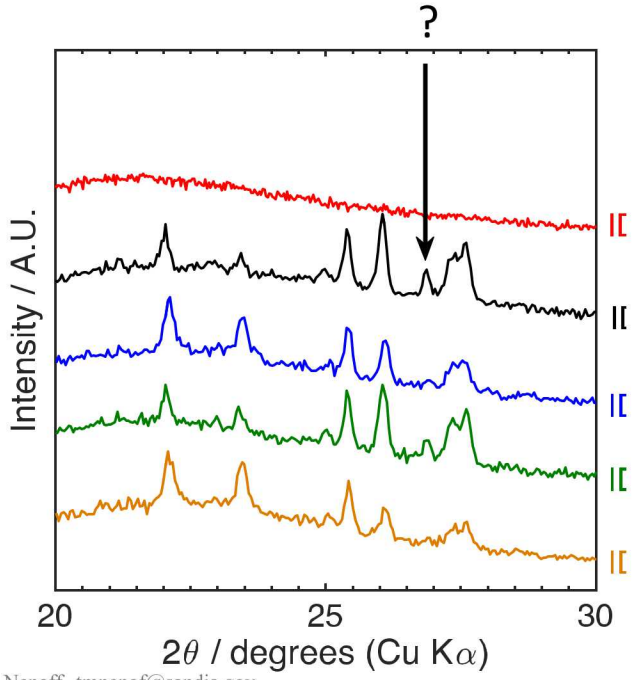


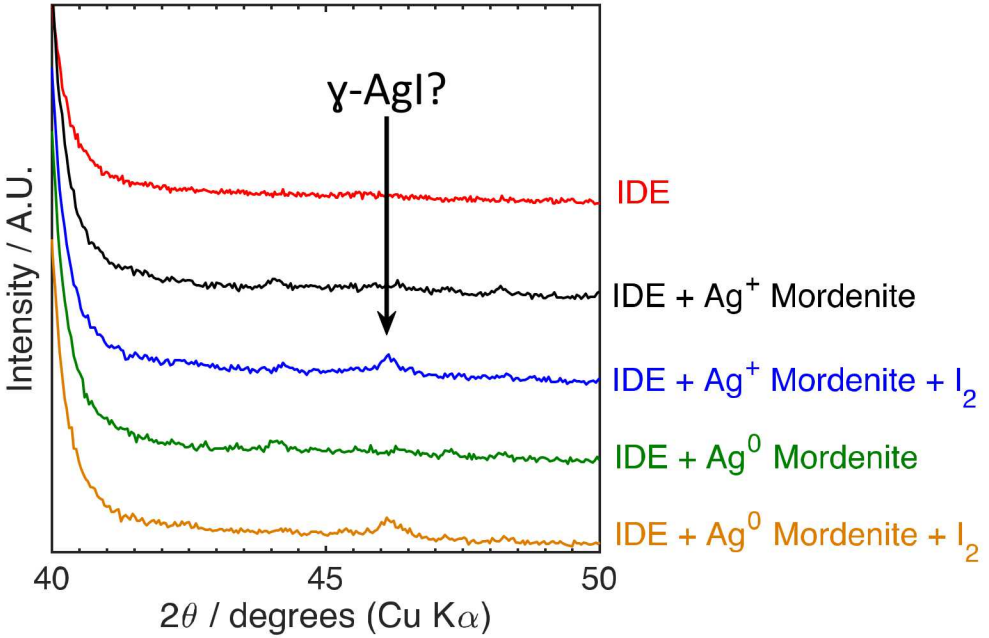

# Diffuse Reflectance FT-IR

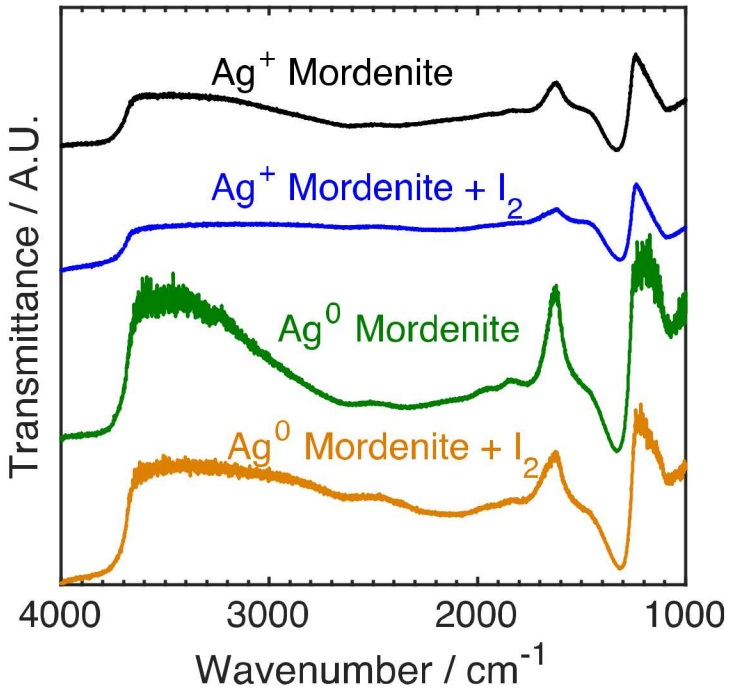


No appreciable change in IR observed upon adding $I_2$ to $Ag^+$ or $Ag^0$ - MOR

# $I_2$@ZIF-8 Pressure-Induced Amorphization of Trapped Gases: Enhanced Retention

Secure consolidated interim storage before incorporation into a long term waste form.

Chapman, Nenoff, et.al., *JACS* **2011**, *133*(46), 18583.

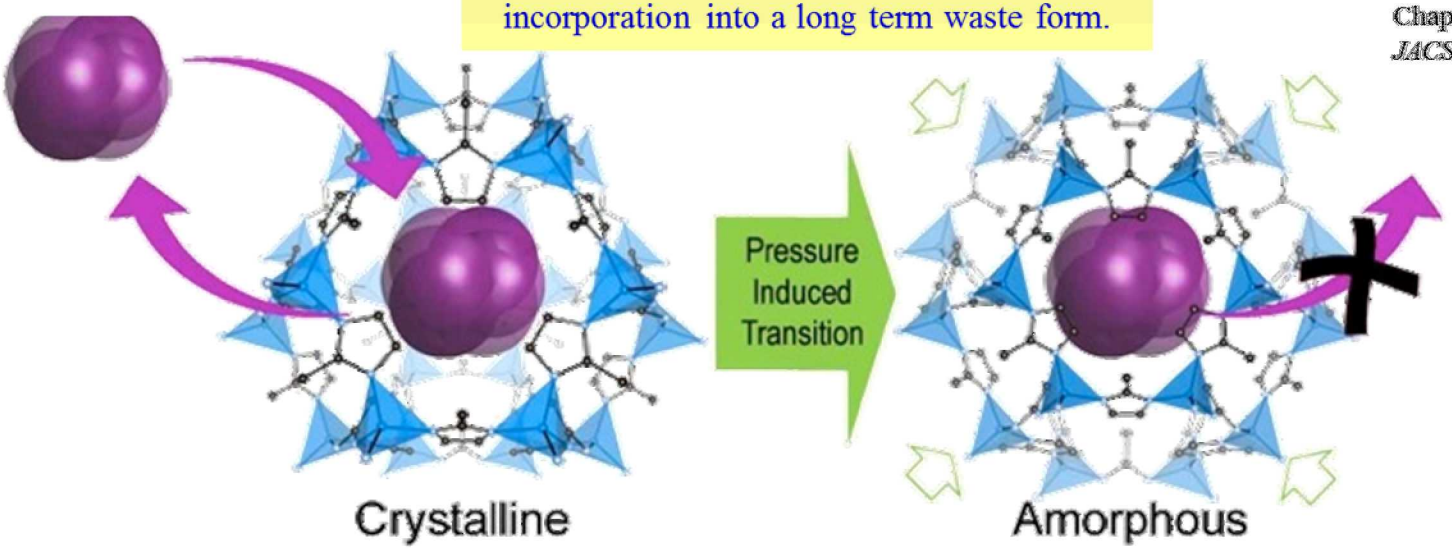


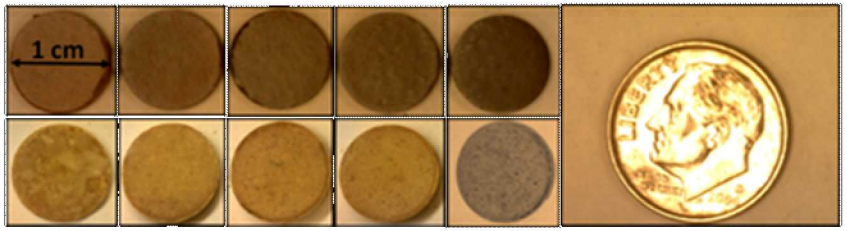


Crack free pellets of iodine loaded ZIF-8 powders were obtained by applying uniaxial mechanical pressure.

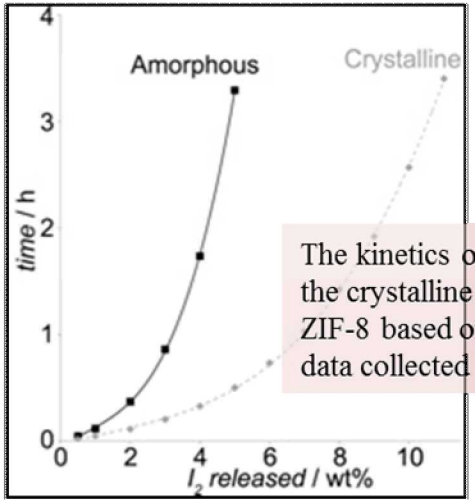


The kinetics of $I_2$ release from the crystalline and amorphized ZIF-8 based on isothermal TGA data collected at 200°C, 4hours

# MOF/Sensor Temperature Dependence

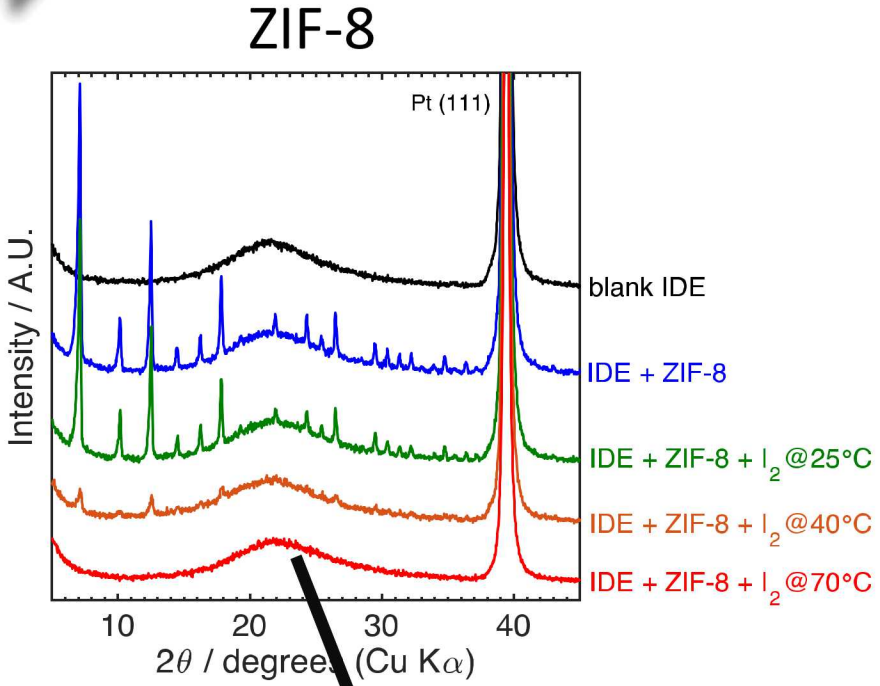


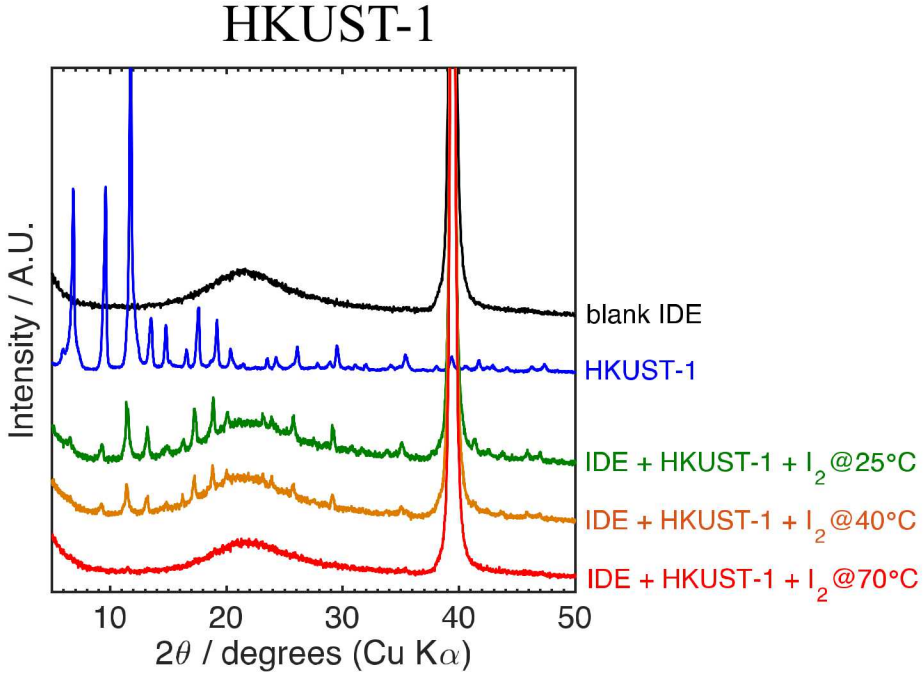


Retention of Iodine in MOF due to SHORT range crystallinity

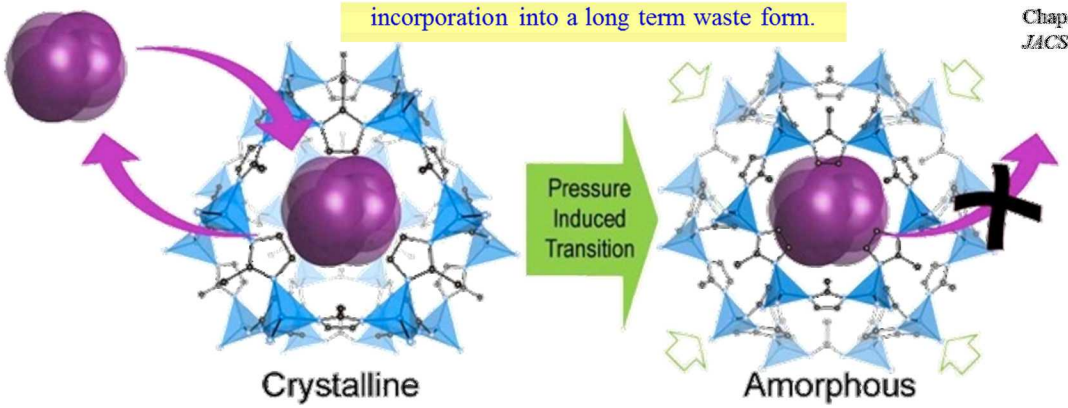

# Iodine ($I_2$) Sensor with HKUST-1


as-received

HKUST-1 + $I_2$ 40 °C

HKUST-1 + $I_2$ 70 °C

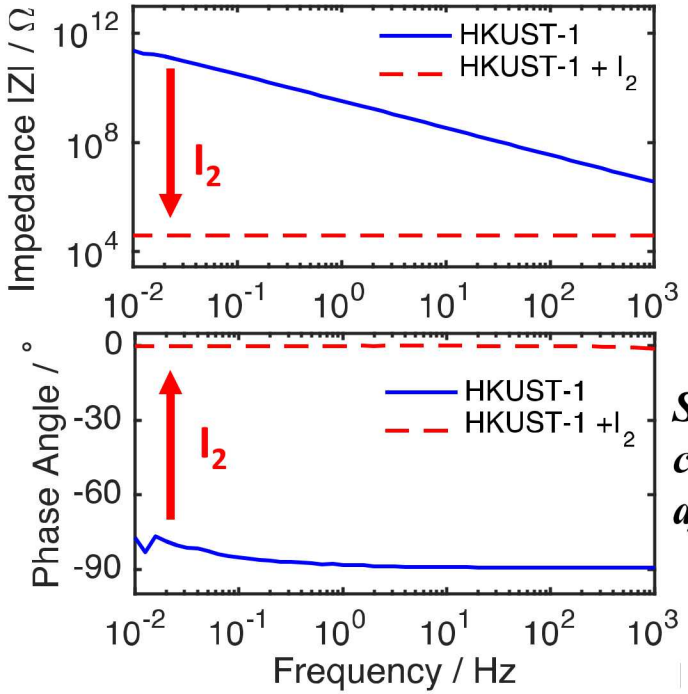


***>6 order magnitude decrease in impedance 70 °C, 30 min $I_2$ exposure***

***Sensor changes from ideal capacitor to ideal resistor after $I_2$ sorption.***

| Loading Temperature (˚C) | "Empty MOF" Device impedance (GΩ) | "$I_2$-Loaded MOF" Device impedance (GΩ) | % Change |
|---|---|---|---|
| Room temp. | 105 | 21 | -80% |
| 40 | 106 | 4.73 | -96% |
| 70 | 99.0 | 38.8 **kΩ** | -100% |

|Z| recorded at 15 mHz. 10 mV AC. 0 V DC.

# Irradiations stability testing of SNL Waste Forms at Sandia Gamma Irradiation Facility (GIF)

Dose rates:

-long-term exposure/low dose:

0.1 Rads/sec, with an overall dose of 2.59 x $10^5$ Rads (2218Gy)

-short-term exposure/high dose:

800 Rads/sec, 1 x $10^6$ Rads (10,000 Gy)

Samples tested include:

EG 2922 Glass (550°C), 87.5Glass/12.5$SiO_2$

80Glass/20AgI-MOR/10Ag

ZIF-8 (MOF), ZIF-8/$I_2$

HKUST-1(MOF), HKUST-1/$I_2$, Glass/HKUST-1/$I_2$

Bi-I-O

Examples of MOF irradiation studies:

90 wt.% $I_2$-loaded ZIF-8 before (red) & after (blue) irradiation: long-term exposure/low dose

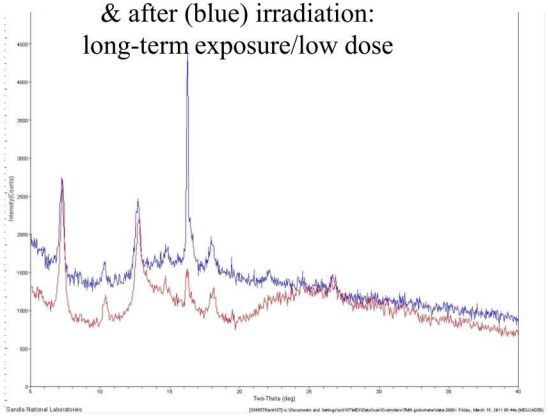

$I_2$-loaded (≈100wt%) HKUST-1 before (red) & after (blue) irradiation: long-term exposure/low dose

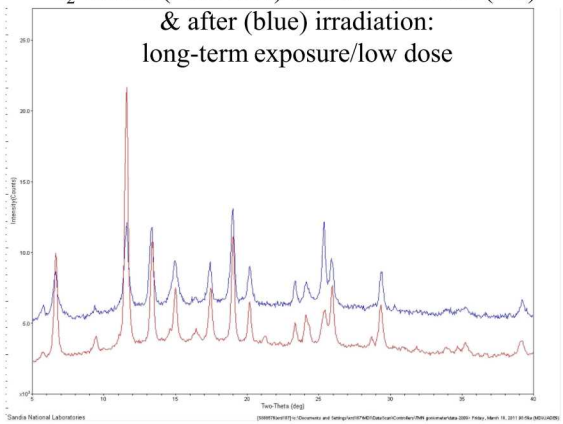

GCM-4 before (red) & after long-term exposure/low dose (blue) irradiation, added short-term exposure/high dose (purple)
GCM-4: EG2922/$I_2$-HKUST-1/Ag

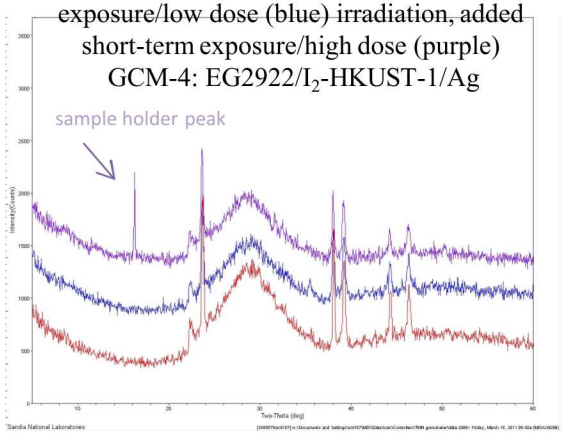


No structural changes as seen by XRD or in PCT responses of any samples. This radiological characterization is a good approximation of an adequately shielded long-term disposal environment.*

*R. H. Jones, Radiation Effects; A Compilation of Special Topic Reports, prepared for the Waste Package Materials Performance Peer Review submitted to U.S. DOE and Bechtel SAIC Company, 18-1 (2002).